

10-19-2005

Torsion-Induced Pressure Distribution Changes in Human Intervertebral Discs: an *In Vitro* Study

Brenda Kay Yantzer
University of South Florida

Follow this and additional works at: <https://digitalcommons.usf.edu/etd>



Part of the [American Studies Commons](#)

Scholar Commons Citation

Yantzer, Brenda Kay, "Torsion-Induced Pressure Distribution Changes in Human Intervertebral Discs: an *In Vitro* Study" (2005). *USF Tampa Graduate Theses and Dissertations*.
<https://digitalcommons.usf.edu/etd/924>

This Thesis is brought to you for free and open access by the USF Graduate Theses and Dissertations at Digital Commons @ University of South Florida. It has been accepted for inclusion in USF Tampa Graduate Theses and Dissertations by an authorized administrator of Digital Commons @ University of South Florida. For more information, please contact digitalcommons@usf.edu.

Torsion-Induced Pressure Distribution Changes in Human Intervertebral Discs:
an *In Vitro* Study

by

Brenda Kay Yantzer

A thesis submitted in partial fulfillment
of the requirements for the degree of
Master of Science in Biomedical Engineering
Department of Chemical Engineering
College of Engineering
University of South Florida

Major Professor: Wesley M. Johnson, Ph.D.
Thomas B. Freeman, M.D.
William E. Lee III, Ph.D.

Date of Approval:
October 19, 2005

Keywords: Intradiscal pressure, pressure transducer, nucleus pulposus, lumbar spine, biomechanics, spinal load

© Copyright 2005, Brenda Kay Yantzer

Table of Contents

List of Tables	iii
List of Figures	iv
Abstract	ix
Chapter One: Introduction	1
1.1 Significance	1
1.2 Background	2
1.2.a Anatomy of the Human Spine	2
1.2.b Comparative Porcine and Human Anatomy	4
1.2.c The Degenerative Process	4
1.2.d Research Objective	6
1.3 Current Intervertebral Disc Model	7
1.4 Intradiscal Pressure History	8
1.5 Pressure Measurements	8
1.6 Apparatus	9
Chapter Two: Materials and Methods	10
2.1 Cadaveric Material	10
2.2 Experimental Technique	11
2.3 Validation	13
2.4 The Effect of Different Torsion Torques on Pressure and Disc Height	14
2.5 Statistical Analysis	14
Chapter Three: Results	15
3.1 Tissue Degradation During Testing	15
3.2 The Effect of Pressure Probe Orientation	15
3.3 The Effect of Disc Degeneration on Pressure	16
3.4 The Effect of Pressure with Applied Torsion	16
3.5 The Effect of Disc Height with Applied Torsion	17
3.6 The Correlation of Pressure and Disc Height with Torsion	19
Chapter Four: Discussion	20
4.1 Discussion of Results	20
4.2 Limitations	21

4.2.a	Sample Size and Variability	21
4.2.b	Testing	22
Chapter Five:	Future Work	23
5.1	Research	23
5.1.a	Sample Size and Variability	23
5.1.b	Testing	23
5.2	Applications	25
References		26
Appendices		31
Appendix A	- Tables	32
Appendix B	- Figures	40

List of Tables

Table 1 - Cadaveric Specimen Record	32
Table 2 - Mean Pressures of 6 FSU and 6 DBU Specimens (n=6)	33
Table 3 - Compiled Pressure Versus Torque ANOVAS for 6 FSU and 6 DBU Specimens (n=6)	34
Table 4 - Mean Pressures of 4 FSU and 4 DBU Specimens (n=4)	35
Table 5 - Compiled Pressure Versus Torque ANOVAS for 4 FSU and 4 DBU Specimens (n=4)	36
Table 6 - Mean Height Differences of all 6 FSU and 6 DBU Specimens	37
Table 7 - Compiled Height Versus Torque ANOVAS for 6 FSU and 6 DBU Specimens	38
Table 8 - Linear Regression Analysis	39

List of Figures

Figure 1 - A. Cannula, B. Needle and C. Pressure Probe	40
Figure 2 - X-ray of FSU UF05H007	41
Figure 3 - MRI of Lumbar Spine UT04K009	42
Figure 4 - MRI of Lumbar Spine UF05B003	43
Figure 5 - Disarticulation of a Spine into an FSU (Functional Spine Unit)	44
Figure 6 - Potted L2 Vertebral Body	45
Figure 7 - Potted L1 Vertebral Body	46
Figure 8 - X-ray of FSU UF05H007 with Screws	47
Figure 9 - Axial Compression of an FSU in the MTS Machine	48
Figure 10 - Insertion of the A. Cannula and B. Needle into an FSU	49
Figure 11 - A. Pressure Gauge and B. Pressure Probe	50
Figure 12 - Pressure of FSU UT04K009. Taken at 0 Nm Torque at the Start and End of the Testing Protocol	51
Figure 13 - Pressure of DBU UT04K009. Taken at 0 Nm Torque at the Start and End of the Testing Protocol	51
Figure 14 - Probe Orientations of DBU UJ04L015 at 0 Nm Torsion Torque	52
Figure 15 - Probe Orientations of DBU UJ04L015 at 0.5 Nm Torsion Torque	52
Figure 16 - Probe Orientations of DBU UJ04L015 at 1.0 Nm Torsion Torque	52
Figure 17 - Probe Orientations of DBU UJ04L015 at 2.0 Nm Torsion Torque	52
Figure 18 - Pressure of FSU UT04K009 at Different Torques	53

Figure 19 - Pressure of DBU UT04K009 at Different Torques	53
Figure 20 - Pressure of FSU UJ04L015 at Different Torques	54
Figure 21 - Pressure of DBU UJ04L015 at Different Torques	54
Figure 22 - Pressure of FSU UJ04J002 at Different Torques	55
Figure 23 - Pressure of DBU UJ04J002 at Different Torques	55
Figure 24 - Pressure of FSU UF05H007 at Different Torques	56
Figure 25 - Pressure of DBU UF05H007 at Different Torques	56
Figure 26 - Pressure of FSU UM05H007 at Different Torques	57
Figure 27 - Pressure of DBU UM05H007 at Different Torques	57
Figure 28 - Pressure of FSU UF05B003 at Different Torques	58
Figure 29 - Pressure of DBU UF05B003 at Different Torques	58
Figure 30 - Pressure Versus Torque of 6 FSU's and 6 DBU's (n=6). Results Shown in Mean \pm Standard Deviation	59
Figure 31 - Pressure Versus Torque of 4 FSU's and 4 DBU's (n=4). Results Shown in Mean \pm Standard Deviation	60
Figure 32 - FSU Two Hour Creep Curves	61
Figure 33 - DBU Two Hour Creep Curves	62
Figure 34 - Combined FSU and DBU Two Hour Creep Curves	63
Figure 35 - Continuous FSU Creep Curves with Two Hour Creep and Testing	64
Figure 36 - Continuous DBU Creep Curves with Two Hour Creep and Testing	65
Figure 37 - Axial Displacement of FSU UT04K009	66
Figure 38 - Axial Displacement of FSU UT04K009 with Logarithmic Trendline	66

Figure 39 - Axial Displacement of FSU UT04K009 with Creep Only	66
Figure 40 - Magnitude of the Height Differences of FSU UT04K009	66
Figure 41 - Axial Displacement of DBU UT04K009	67
Figure 42 - Axial Displacement of DBU UT04K009 with Logarithmic Trendline	67
Figure 43 - Axial Displacement of DBU UT04K009 with Creep Only	67
Figure 44 - Magnitude of the Height Differences of DBU UT04K009	67
Figure 45 - Axial Displacement of FSU UM05H007	68
Figure 46 - Axial Displacement of FSU UM05H007 with Logarithmic Trendline	68
Figure 47 - Axial Displacement of FSU UM05H007 with Creep Only	68
Figure 48 - Magnitude of the Height Differences of FSU UM05H007	68
Figure 49 - Axial Displacement of DBU UM05H007	69
Figure 50 - Axial Displacement of DBU UM05H007 with Logarithmic Trendline	69
Figure 51 - Axial Displacement of DBU UM05H007 with Creep Only	69
Figure 52 - Magnitude of the Height Differences of DBU UM05H007	69
Figure 53 - Axial Displacement of FSU UJ04L015	70
Figure 54 - Axial Displacement of FSU UJ04L015 with Logarithmic Trendline	70
Figure 55 - Axial Displacement of FSU UJ04L015 with Creep Only	70
Figure 56 - Magnitude of the Height Differences of FSU UJ04L015	70
Figure 57 - Axial Displacement of DBU UJ04L015	71
Figure 58 - Axial Displacement of DBU UJ04L015 with Logarithmic Trendline	71
Figure 59 - Axial Displacement of DBU UJ04L015 with Creep Only	71

Figure 60 - Magnitude of the Height Differences of DBU UJ04L015	71
Figure 61 - Axial Displacement of FSU UJ04J002	72
Figure 62 - Axial Displacement of FSU UJ04J002 with Logarithmic Trendline	72
Figure 63 - Axial Displacement of FSU UJ04J002 with Creep Only	72
Figure 64 - Magnitude of the Height Differences of FSU UJ04J002	72
Figure 65 - Axial Displacement of DBU UJ04J002	73
Figure 66 - Axial Displacement of DBU UJ04J002 with Logarithmic Trendline	73
Figure 67 - Axial Displacement of DBU UJ04J002 with Creep Only	73
Figure 68 - Magnitude of the Height Differences of DBU UJ04J002	73
Figure 69 - Axial Displacement of FSU UF05H007	74
Figure 70 - Axial Displacement of FSU UF05H007 with Logarithmic Trendline	74
Figure 71 - Axial Displacement of FSU UF05H007 with Creep Only	74
Figure 72 - Magnitude of the Height Differences of FSU UF05H007	74
Figure 73 - Axial Displacement of DBU UF05H007	75
Figure 74 - Axial Displacement of DBU UF05H007 with Logarithmic Trendline	75
Figure 75 - Axial Displacement of DBU UF05H007 with Creep Only	75
Figure 76 - Magnitude of the Height Differences of DBU UF05H007	75
Figure 77 - Axial Displacement of FSU UF05B003	76
Figure 78 - Axial Displacement of FSU UF05B003 with Logarithmic Trendline	76
Figure 79 - Axial Displacement of FSU UF05B003 with Creep Only	76
Figure 80 - Magnitude of the Height Differences of FSU UF05B003	76

Figure 81 - Axial Displacement of DBU UF05B003	77
Figure 82 - Axial Displacement of DBU UF05B003 with Logarithmic Trendline	77
Figure 83 - Axial Displacement of DBU UF05B003 with Creep Only	77
Figure 84 - Magnitude of the Height Differences of DBU UF05B003	77
Figure 85 - Normalized Data Versus Time of FSU UT04K009	78
Figure 86 - Normalized Data Versus Time of DBU UT04K009	79
Figure 87 - Normalized Data Versus Time of FSU UM05H007	80
Figure 88 - Normalized Data Versus Time of DBU UM05H007	81
Figure 89 - Normalized Data Versus Time of FSU UJ04L015	82
Figure 90 - Normalized Data Versus Time of DBU UJ04L015	83
Figure 91 - Normalized Data Versus Time of FSU UJ04J002	84
Figure 92 - Normalized Data Versus Time of DBU UJ04J002	85
Figure 93 - Normalized Data Versus Time of FSU UF05H007	86
Figure 94 - Normalized Data Versus Time of DBU UF05H007	87
Figure 95 - Normalized Data Versus Time of FSU UF05B003	88
Figure 96 - Normalized Data Versus Time of DBU UF05B003	89
Figure 97 - Differential Height Versus Torque of 6 FSU's and 6 DBU's (n=6). Results Shown in Mean \pm Standard Deviation	90

**Torsion-Induced Pressure Distribution Changes in Human Intervertebral
Discs: an *In Vitro* Study**

Brenda Kay Yantzer

ABSTRACT

Introduction. To test the effects of torsion torques on intradiscal pressure and disc height in human lumbar specimens.

Methods. Six human lumbar cadaveric functional spine units (FSU) were loaded in the neutral position with 600 N compression. Nucleus pressure measurements were obtained at 0 Nm, 0.5 Nm, 1.0 Nm and 2 Nm torsion torque. Posterior elements were removed and pressure measurements were repeated at the same torsion torques for the disc body unit (DBU). The pressure in the nucleus was measured by pulling a pressure probe through the disc along a straight path in the midsagittal plane.

Results. There was no statistically significant difference of nucleus pressure or intervertebral disc height with different torsion torques among or between the FSU's and DBU's. However, a disc height increase ranging from 0.13 mm to 0.16 mm occurred with the insertion of a 1.85 mm diameter cannula.

Conclusions. Small torsion torques showed no significant difference in intradiscal pressures or disc heights. Disc height increases were seen with the insertion of the cannula that could lead to methods of disc height restoration.

Chapter One: Introduction

1.1 Significance

Low back pain (LBP) is a widespread problem in society, both in occurrence and economics.^{28,41} Chronic LBP affects more than five million Americans each year and is the second most common reason for lost workdays in adults under the age of 45.^{1,41} Studies have indicated that long periods of awkward postures and highly repetitive activities have been associated with LBP.^{10,28} The pain is often severe and debilitating and it is estimated that more than \$50 billion is spent annually on the lower back.¹ The causes for back pain include disease, trauma and degeneration due to age. These causes can be related to the spine (intervertebral disc and facet joints) or can be myofascial (muscles and fasciae). Specifically, degeneration of the intervertebral disc (IVD) is a major cause of pain, where the spine suffers diminished mechanical functionality due to dehydration of the nucleus pulposus within the disc.^{5,21,29} The pain caused by the IVD, called discogenic pain, is the number one disease contributing to lost workdays and is an indication for fusion surgery.⁴¹ While only 5 percent of all LBP is discogenic, it accounts for 95 percent of surgeries for back pain.

Small intervertebral movements such as during walking appear to reduce low back pain and have been hypothesized to prevent degenerative changes in the intervertebral disc.³⁷ These various intervertebral movements include flexion, extension, lateral bending and torsion. Previous studies on porcine specimens have suggested that small torsion rotations have an effect on disc height.³⁷ In a previous research study, it was proposed that torsion torque could affect the pattern of fluid loss and depressurization of the intervertebral disc that occurs in daily loading, and therefore have an instantaneous effect on disc height and

intradiscal pressure.^{17,37} The previous research by van Deursen tested only porcine disc body units (DBU's: motion segments with posterior elements removed), to determine if torsion torque had an affect on intradiscal pressure and disc height. Only DBU's were used because it allowed fixation of the specimens into the testing apparatus. The motivation behind the current research was to extend and expand the previous research to include testing not only DBU's in human specimens, but testing functional spine units (FSU's: motion segments with posterior elements intact) as well. The reason behind testing FSU's was because those results would have more clinical relevance since people have posterior elements (at least prior to a surgical operation). The objective of this research was to biomechanically test the hypothesis that small torsion torques cause decreased pressure in the nucleus pulposus while increasing disc height in the human lumbar spine.

1.2 Background

1.2.a Anatomy of the Human Spine

The spine performs 3 significant roles including: strength for the skeleton (load-bearing); provision of movement; and protection of the neural elements (spinal cord, nerve roots) from trauma.^{21,28,29} The adult spinal column consists of 7 cervical vertebrae, 12 thoracic vertebrae, 5 lumbar vertebrae, 5 fused sacral vertebrae and 3 to 4 fused coccygeal segments.²¹ Motion occurs in 6 degrees of freedom: rotational and translational motion in 3 different planes. By the right hand Cartesian coordinate system and by a semi-arbitrary convention, motion is allowed by rotation about the x-axis (flexion-extension or lateral bending), rotation about the z-axis (torsion), translation about the z-axis (axial compression), and translation about the x and y axes (shear motion in the x and y axes, respectively).

The vertebrae provide anterior support and structure of the spine (bearing about 80% of the spinal load), while the facet joints afford posterior stability

(bearing about 20% of the spinal load).^{21,29,39} Intervertebral discs lie in between the vertebrae and are responsible for transmitting loads (compressive, tensile and shear, in short duration loading and low magnitude loading) and providing shock absorbance (dissipating energy by converting kinetic energy into heat over a longer period of time and over more components to dampen loading affects).^{28,39} In addition, the discs allow flexibility and motion of the spinal column.^{28,29,39}

Intervertebral discs are made up of two parts including a gelatinous nucleus pulposus surrounded by a strong fibrous and cartilaginous annulus fibrosus.^{1,4,15,29} The primary structural components that make up both the nucleus and the annulus include collagens and proteoglycans. Each component is very important because each offers unique structural integrity and stability to the disc.^{4,6,12} Specifically, proteoglycans interact with water to provide stiffness and compressive resilience to the tissue, while collagens provide tensile strength to the tissue.^{4,6,12}

The nucleus is composed of hydrophilic proteins called proteoglycans and collagen protein fibers that are arranged in an irregular manner, forming a gel matrix.^{4,6,12,29} The nucleus is located in the center of the disc and is almost 90% water in young individuals.^{12,29} The water content is highest at birth but decreases to 70% with degeneration due to age.

The annulus is the outer portion of the disc. It is comprised of multiple layers of collagen fibers that are arranged in alternating directions (30° to the disc plane and 120° to each other), which are placed under tension when the nucleus absorbs water and swells.^{6,18,21,25,29} The annulus has a higher water content in younger people, about 78%, but decreases to about 70% with degeneration due to age.^{29,39}

There are two layers of vertebral cartilage endplates, located above and below the disc, that allow for the exchange of nutrients and water. Since IVD's are not vascularized, except at birth, this exchange mechanism is very important.^{7,28}

The amount of water in the nucleus is dependent on its chemical composition in addition to the external load on the disc.^{2,3,9,24} When there is a high load on a disc, the pressure inside the nucleus increases, forcing water out of the disc and into the endplate. There, the capillaries can remove the water. When lying down, the nucleus pressure decreases and the water returns. In effect, a pump is created resulting in circulation that brings nutrition into the disc while removing the products of metabolism out of the disc.^{7,28,34}

The size of the spinal canal has been found to correlate with the occurrence of back pain.²¹ Nerve roots exit at each vertebral level. They pass laterally through openings called neuroforamina, travel under the facet joints and superior to the disc.²¹ As the disc height decreases, the neuroforamina decreases as well causing the two vertebral bodies to come closer together. Branches of the sinuvertebral nerve innervate the outer layers of the annulus, and as the vertebral bodies come together, the nerve begins to be pinched.²¹ Back pain is thought to originate from the stimulation of this nerve.

1.2.b Comparative Porcine and Human Anatomy

Animal model fidelity is an important issue concerning disc degeneration and bone morphology when comparing human spines to animal spines. In general, the porcine vertebrae are smaller than the human vertebrae in all dimensions, and have similar ligamentous structure and facet joint orientation.^{31,43} In addition, compressive and shear stiffness values of porcine specimens are comparable to human specimens.⁴³ Therefore, porcine spines may be useful for studying and comparing human spines to an animal model.

1.2.c The Degenerative Process

Degeneration of the spine is a prevalent problem that generally advances with age, although its occurrence is not restricted to only the elderly.²⁸ Degenerations of the spine are the leading cause of pain, altered function and

deformity.^{5,28} Degeneration of the IVD is a normal physiologic process associated with age, and usually begins around the age of 30.³² At that age, there are gradual changes in the types of proteoglycans present and therefore the overall water content of the IVD changes similarly as well.²⁹ In fact, degeneration may be accelerated with excessive loading of the disc.^{32,39} The change in water content on the disc decreases the load experienced by the nucleus, while increasing the load experienced by the annulus.³⁹ As the nucleus shrinks, the changes in load distribution have occurred and can result in tears, cracks, or fissures in the annulus.^{16,19} The defects usually occur in the posterior and posterolateral regions of the annulus, which can proliferate and cause the nuclear material to migrate from the center to the periphery of the disc.^{16,19} The expansion of the nucleus through the annular layers causes stretching and delamination of these layers and causes back pain due to stimulation of the sinuvertebral nerve.¹⁹ A complete extrusion of the nucleus through all of the layers of the annulus can result, causing a disc herniation.¹⁹ The nucleus that was protected from the vascular system and immune system, is now exposed to it and it causes an inflammatory response to occur.²¹ In addition, the herniated disc may compress a nerve root causing severe pain. The biomechanical properties of the disc including the ability to transmit load, absorb shock and allow motion, change significantly with degeneration due to age.³⁹

Because of aging, the disc desiccates and becomes less compressible. Additionally, the vertebral endplates become sclerotic, less porous, and less able to transport nutrients to the disc.³⁴ Since diffusion is the main mechanism of transport through the disc, when the disc is unable to obtain as many nutrients or remove waste products efficiently, the pump action is largely lost.³⁴ Also, an acidic environment is created when the metabolic end-products accumulate.³⁴ There may be an inflammatory response to the site as well. Both the acidity and inflammatory response cause pain.

As a result of the desiccation of the disc, there is a reduction in the height of the disc. The annular fibers bow out, and this leads to thecal sac and nerve

root compression. Furthermore, spinal stability is altered. Stability is changed when the discs are no longer capable of supporting the weight of the spine, and facets and ligaments are forced to support more weight. The facets and ligamentum flavum can become hypertrophied, leading to less space for the thecal sac and nerve roots, causing neural compression and pain.²¹ With the degenerating facets, the discs experience additional shear stress, and become further degraded. This causes increased pain, spinal instability and spinal misalignment.²⁶ Since a reduction in disc height is a major source of pain for millions of people, treatments or surgical operations should focus on restoration of disc height. In order to restore disc height, it is critical to understand what motions could contribute to a disc height change.

1.2.d Research Objective

The hydrostatic pressure within the nucleus pulposus is a key component for the ability of the IVD to support physiologic loads.³⁶ Horst and Brinkmann studied the distribution of axial stress on the vertebral body end plate by using pressure transducers in IVD's of cadaveric lumbar spine segments.^{13,28} McNally and Adams used intradiscal stress profilometry to determine the pressure distributions within the human IVD.^{3,24} Van Deursen found a decrease in intradiscal pressure and an increase in disc height with increased torsion in the porcine DBU.³⁷ Although intradiscal pressures and the affects of aging, degeneration and loading have been studied and modeled, there is little information on disc heights and intradiscal pressures related to torsional torques applied to the human lumbar spine.^{20,24,27,35} The purpose of the present research was to gain a more detailed understanding of height and intradiscal pressure changes that may accompany torsional torques, by measuring pressure distributions within loaded human cadaveric lumbar intervertebral discs.

1.3 Current Intervertebral Disc Model

The IVD is subjected to many different loads in everyday life. It is a complex mechanical system that is assumed to distribute compressive stresses evenly between adjacent vertebrae because the nucleus pulposus and inner annulus act as a pressurized fluid that does not vary with location or direction.^{2,3,37} According to Adams et al,³ the nucleus acts as a sealed hydraulic system, where the fluid pressure rises substantially when volume is increased (by fluid injection) and falls when volume is decreased (by surgical excision or endplate fracture).^{2,3,37} The IVD, therefore, is able to withstand compression because of the swelling pressure exerted by the nucleus pulposus which is constrained radially by the annulus fibrosus.^{14,28} Previous loading and disc degeneration can cause peaks in the recorded pressure.

Previous authors have reported that small axial torsion rotations of the porcine disc caused a decrease of pressure in the nucleus pulposus.³⁷ Furthermore, the pressure reduction in the nucleus under torsional rotations was related to an increase of disc height.³⁷ An increase of disc height would explain the pain reduction patients with low back pain can achieve through small rotations.³⁷ The increase in disc height would decrease facet joint loading and increase the foraminal space, thus minimizing pain.³⁷ However, the results were obtained from porcine specimens without posterior elements. Porcine specimens generally show no signs of IVD degeneration and posterior elements are important because of their clinical relevance in the human population.

To determine if IVD condition and posterior elements affected pressures and disc heights with different torsion torques in human specimens, torsion torques were applied to human cadaveric specimens. The pressure profiles were measured through the human IVD in neutral position, 0.5 Nm, 1.0 Nm and 2.0 Nm of torsion (up to 1.5° right torsion), as described by McNally and Adams et al.^{3,24} Both FSU's and DBU's were tested in human cadaveric specimens. Those torsion torques were within the physiologic range (5-7° range of motion) to prevent damage to the facet joints and remain within the range used in the

previous porcine research.^{37,39} Disc heights were measured and recorded to determine if there was a significant change with the application of different torsion torques.

1.4 Intradiscal Pressure History

Most of the present knowledge related to intradiscal pressures was produced from studies by Nachemson.²⁷ These pressure measurements were performed in the 1960's and 1970's in cadaveric IVD's using a polyethylene-covered disc pressure probe connected to an external electromanometer.^{27,33,36} Nachemson and collaborators went on to measure IVD pressures in vivo for different body postures and while performing a variety of lifting maneuvers.²⁷ Their measurements revealed that the nucleus pulposus behaved as a hydrostatic fluid.^{2,3,27,36} Although useful data was recorded, the method had many disadvantages including the probe having a very cumbersome assembly and calibration, as well as the probe displaying poor dynamic characteristics.²⁷ Additionally, high pressures could damage the probe.²⁷ A new method of measuring intradiscal pressure was developed that used a more advanced pressure sensor with strain gauges.⁴¹ This method minimized those problems.

1.5 Pressure Measurements

There are different techniques for measuring nuclear pressure including simple liquid-coupled systems to strain-gauge transducers mounted on the ends.²⁴ These techniques have demonstrated that the center of the nucleus behaves as a fluid, except in discs that are severely degenerated.²⁴ There are no measurements, however, that report the stress in FSU's compared to DBU's in specimens with and without disc degeneration. Pressure measurements could be obtained by inserting a pressure probe into the disc and varying its position and orientation in several different specimens, with and without posterior elements, and recording the pressure continuously.^{24,30}

A probe capable of measuring stresses within a disc was developed and tested by McNally and Adams et al.^{3,24} The probe measured the component of compressive stress perpendicular to its sensitive surface, the sensing element, and was mounted on the side of the probe so it could be rotated to measure the component of stress in different orientations. The gross mechanical properties of the disc were not adversely affected as the diameter (1.27 mm) of the probe was small and could be positioned anywhere within the nucleus or annulus. By moving the probe through the disc, a continuous plot of pressure against time could be obtained along any path and a complete plot of pressure measurements within the disc under different parameters could be constructed.^{3,23,24}

1.6 Apparatus

The pressure probe (OrthoAR Model No: 0571521-57, Medical Measurements Incorporated, Hackensack, NJ) used in this research consisted of a pressure sensor mounted on a 125 mm long, 1.27 mm diameter stainless steel probe (Figure 1, C.) The finish at the end of the probe was rounded and the sensor was located proximal to the end. The probe was connected to a 50 cm long, 3.17 mm outer diameter cable constructed from an ultraflex catheter material that terminated in a lightweight connector. The catheter material was flexible to reduce tension while making measurements.

The operating principle of the pressure probe was based on the piezoresistance of semiconductor strain gauges.²⁴ It was a microelectromechanical system (MEMS) device using a full bridge gauge to form a Wheatstone bridge. The piezoresistors generated an output voltage proportional to the applied pressure.

The pressure transducer had a full scale range of 0-2 MPa with a burst pressure of 3.5 MPa and could withstand temperatures of 25°C to 37°C.

Chapter Two: Materials and Methods

2.1 Cadaveric Material

Ten human lumbar cadaveric spines were obtained at routine postmortems from individuals who had been mobile prior to death and had no history of disease known to affect the biomechanical properties of the spine.²⁴ The ages of the individuals ranged from 38 to 65 years (mean, 50 years; Table 1). The ten specimens were radiographed using magnetic resonance imaging (MRI; GE LX, High Field 1.5 Tesla Scanner) and X-rayed using the digital Faxitron (Model No: MX-20, Wheeling, Illinois) to determine if any bone, disc, or facet joint abnormalities were present. Figure 2 was an example of an X-ray taken of specimen UF05H007. Figures 3 and 4 demonstrated examples of MRI's taken of spines UT04K009 and UF05B003, respectively, before disarticulation. Four specimens revealed either bridging osteophytes across the disc space of interest, a collapsed disc space or vertebral compression fractures, causing them to be excluded from testing. The remaining 6 specimens were stored in a freezer at -17 °C for up to 6 months before disarticulation. Previous research by Dhillon, Bass and Lotz reported that freezing specimens for a reasonable amount of time using a typical method of freezing and thawing did not significantly effect the properties of human lumbar discs.⁸ Each specimen was then thawed at 7 °C and disarticulated into an L1-L2 FSU (functional spine unit) consisting of two adjacent vertebral bodies and the IVD (intervertebral disc) between them (Figure 5). Excess musculature was removed from each FSU but caution was taken to keep the disc, ligaments and facet joint capsules intact. After disarticulation, each specimen was potted with a mildly exothermic polyester resin using 4 X 4 inch potting frames on either end (Figures 6 and 7). Screws were used to secure the vertebral bodies into the resin and additional x-rays were taken with a digital X-

ray unit (Faxitron, Model No: MX-20, Wheeling, Illinois) to confirm that no screws had penetrated the disc-space (Figure 8). The specimens were routinely sprayed with saline during tissue preparation and potting to prevent desiccation.

One specimen at a time was disarticulated, prepared and potted, while the remaining specimens were kept in the freezer. After each specimen was prepared and was ready to be used, it was thawed and tested immediately. Each specimen was tested during a two day period.

2.2 Experimental Technique

The experiment was performed under the University of South Florida, Institutional Review Board requirements. Six L1-L2 human cadaveric lumbar motion segments were tested with and without posterior elements using a servo hydraulic materials testing system (MTS Systems Incorporated, 858 Bionix II, Eden Prairie, MN). The upper framed vertebral body was tightened into a stationary fixture attached to an anti-rotation device and a load cell, while the bottom framed vertebral body was tightened into a fixture attached to the torsion motor (Figure 9). The fixture system allowed axial compression to be continuously applied with and without combined torsional loading. The testing sequence included each FSU being axially compressed for 2 hours, immediately followed by combined axial compression and torsion torque (while taking pressure measurements) for less than 16 minutes (Figures 9 and 10). Subsequent to testing, the posterior elements of each FSU were removed to convert the FSU into a DBU. The same testing protocol was repeated for each of the 6 DBU's.

The water content of an IVD may change postmortem as a result of an extended period of unloading. Therefore, a preliminary creep test was performed on each specimen to normalize the water distribution of the disc.^{2,23} Fluid was squeezed out of the disc by compressing each FSU or DBU for 120 minutes at 600 N, to simulate relaxed standing (Figure 9).^{23,36,38,40,42} It was found in previous studies that simulating muscle forces substantially affects intradiscal

pressure, so 600 N was applied to all specimens for both the creep and torsional tests.^{38,40,42}

Following the creep test, all 6 FSU's and all 6 DBU's were compressed continuously at 600 N, to simulate physiologic loading, while torsion torque was applied at 0 Nm, +0.5 Nm, +1.0 Nm and +2.0 Nm. During each different torsion torque application, pressure measurements were obtained with the pressure probe. Only positive torsional torques were applied because initial testing revealed no significant difference between positive and negative torsion torques. The various positions were achieved by the MTS using MPT software and a custom computer-controlled torsion motor that rotated the lower vertebral body over a specified torque. The duration of each test lasted 15 minutes and 45 seconds. Time, axial force, axial displacement, torsion torque, torsion angle, and intradiscal pressures were recorded by MPT during each test. Creep was a factor that affected each specimen, however, the contribution due to creep was taken into account using a logarithmic function during data analysis.¹¹

The pressure measurements were collected using a pressure probe (Figure 1 C). The pressure probe was introduced into the disc by the following method. A 1.25-mm diameter hypodermic needle (Figure 1 B), surrounded by a 1.85-mm stainless steel cannula (Figure 1 A), was pushed into the anterior annulus in the midsagittal plane of the IVD until it pushed through the posterior annulus (Figure 10). Care was taken to ensure the cannula was parallel to and equidistant from the two vertebral end plates. The needle was removed from the cannula and the pressure probe was inserted. The cannula was pulled back so the transducer tip was exposed to the posterior annulus, and the pressure probe was manually pulled through the disc at a speed of about 2 mm/sec until it emerged from the anterior annulus completely. The pressure-sensitive membrane of the pressure probe was oriented either horizontally or vertically in order to measure the pressures in the horizontal or vertical directions, respectively. The cannula was inserted into the same needle track to reduce alterations of the IVD that could arise from multiple needle sticks. The

measurements were reproducible and did not perturb the tissue to any significant extent.

The pressure probe was calibrated before the start of the experiment and at the end of the testing using a National Institute of Standards and Technology (NIST) certified pressure gauge (Figure 11 A). There was no change in the probe, so any pressure changes that were seen during data collection were due only to pressure changes of the specimen itself and the torsion torque applied, not from changes in the pressure probe.

2.3 Validation

Degradation could be a limiting factor when testing cadaveric specimens. To determine if degradation occurred, a pressure measurement at 0 Nm torsion torque was taken after the other four torsions torques (0 Nm, 0.5 Nm, 1.0 Nm and 2.0 Nm) were applied. The initial pressure measurements taken at 0 Nm and the repeat measurement taken at 0 Nm at the end of the test were compared to determine if there was a significant difference between them. If there was no significant difference between the two 0 Nm measurements, then the testing did not significantly degrade the cadaveric tissues under investigation. The likelihood of specimen degradation occurring under repeated loading prevented the testing of all combinations on each motion segment.

Another problem that could occur during testing is equipment failure. In order to test that the probe did not measure pressure inaccurately, it was calibrated at the beginning and calibrated at the end of testing, and the results were compared. The pressure probe was calibrated using an NIST certified pressure gauge (Figure 11 A). The NIST certified pressure gauge used was a bubble-free, glycerin-filled, nylon-case gauge with a 1% full-scale accuracy. The glycerin gauge was mounted on pipe fittings that were connected to the pressure probe (Figure 11 B). Both the gauge and the probe were connected up to a nitrogen tank pressure source (Figure 11).

2.4 The Effect of Different Torsion Torques on Pressure and Disc Height

Pressure profiles were obtained for all 6 FSU and all 6 DBU specimens while torsion torque was varied independently. Intradiscal pressure and disc height were dependent variables that were recorded and analyzed. Up to 5 pairs of horizontal and vertical pressure profiles were obtained from each motion segment (including FSU's and DBU's). The compressive force applied was 600 N in order to simulate relaxed standing *in vivo*.^{40,42}

2.5 Statistical Analysis

The results from the torsion torques applied to all 6 specimens (FSU's or DBU's) were averaged, including pressures and differential disc heights. Descriptive statistics and single factor analysis of variances (ANOVAS) were performed with pressure (among and between 6 FSU's and 6 DBU's), torsion torque (0 Nm, 0.5 Nm, 1.0 Nm and 2.0 Nm), and differential disc heights (among and between 6 FSU's and 6 DBU's). The null hypothesis was $H_0: \mu_1 = \mu_2$, while the alternative hypothesis was $H_a: \mu_1 \neq \mu_2$. The alpha value of $\alpha = 0.05$, beta value of $\beta = 0.35$, and power of 65% used during data analysis were determined a priori. Results with a p-value of 0.05 or less were considered significant.

As detailed in results section 3.4, 2 specimens were removed from the data analysis because of disc degeneration. The statistical analysis performed on the remaining 4 specimens included descriptive statistics and single factor analysis of variances (ANOVAS) of pressure (among and between 4 FSU's and 4 DBU's), torsion torque (0 Nm, 0.5 Nm, 1.0 Nm and 2.0 Nm), and differential disc heights (among and between 4 FSU's and 4 DBU's). The null hypothesis was $H_0: \mu_1 = \mu_2$, while the alternative hypothesis was $H_a: \mu_1 \neq \mu_2$. An alpha value of $\alpha = 0.05$, beta value of $\beta = 0.5$, and power of 50% were used for the analysis. Results with a p-value of 0.05 or less were considered significant.

Linear regression analysis was performed for pressure versus torsion on $n=6$, for pressure versus torsion on $n=4$ and for height versus torsion on $n=6$.

Chapter Three: Results

3.1 Tissue Degradation During Testing

The mean pressure measurements taken at the beginning and completion of the test protocol at 0 Nm were compared between all functional spine units (FSU's) and all disc body units (DBU's). The results revealed a mean FSU pressure of 0.65 MPa, and no significant difference between the two 0 Nm measurements of the FSU's ($p=0.67$). Similarly, there was no significant difference between the 0 Nm measurements of the DBU's ($p=0.54$), with a mean DBU pressure of 0.57 MPa. An example of the pressures at 0 Nm taken at the beginning and end of the test could be seen in the FSU specimen UT04K009 (Figure 12) and DBU specimen UT04K009 (Figure 13). Since it was demonstrated that there was no significant difference between the pressure measurements taken at 0 Nm before the test started and at 0 Nm at the completion of the test protocol, it is clear that no apparent degradation occurred and testing did not significantly disturb the cadaveric tissues.

3.2 The Effect of Pressure Probe Orientation

The results of intradiscal pressures taken with the pressure probe in horizontal and vertical orientations revealed that there was no significant difference of pressures in the lumbar L1-L2 FSU or DBU. This finding was independent of the torsion torque applied and presence or absence of posterior elements (FSU: 0 Nm $p=0.91$, 0.5 Nm $p=0.95$, 1.0 Nm $p=0.83$, 2.0 Nm $p=0.95$; DBU: 0 Nm $p=0.97$, 0.5 Nm $p=0.84$, 1.0 Nm $p=0.90$, 2.0 Nm $p=0.30$) (Table 2). Figures 14, 15, 16 and 17 demonstrated an example of horizontal and vertical pressures recorded for DBU UJ04L015, at 0 Nm, 0.5 Nm, 1.0 Nm and 2.0 Nm,

respectively. This result confirmed the work done by McNally and Adams, who found that pressure was not affected by pressure probe orientation in healthy specimens without disc degeneration.

3.3 The Effect of Disc Degeneration on Pressure

Intervertebral discs (IVD's) with little or no degeneration revealed pressure graphs very different from those discs with increased degeneration. The graphs of normal IVD's in the FSU's and DBU's revealed a pressure plateau corresponding to the functional nucleus and inner annulus.²⁴ The central region of the nucleus exhibited a hydrostatic pressure, however the 'stepped' portion of the graph correlated to the functional annulus. Graphs from normal discs looked like those in Figures 18-19 (49 year old), Figures 20-21 (38 year old), Figures 22-23 (43 year old) and Figures 24-25 (65 year old) (Table 1). The spikes that could be seen in a few graphs were due to artifacts caused by movement of the probe during its insertion or removal. Graphs from degenerated discs were generally similar to those shown in Figures 26-27 (56 year old) and Figures 28-29 (52 year old) (Table 1). Those graphs were irregular with numerous spikes, and showed no clear-cut region of hydrostatic pressure. It could therefore be said that degeneration of the disc had an apparent effect on intradiscal pressure, which confirmed the research done by McNally and Adams.

3.4 The Effect of Pressure with Applied Torsion

To make quantitative comparisons between pressures recorded from different specimens, mean pressures of the 6 specimens were determined for each torsion torque of the 6 FSU specimens and of the 6 DBU specimens (Figure 30). Descriptive statistics and ANOVAS were performed among and between all 6 FSU's and DBU's and each torsion torque applied (Table 3). Results showed that there was no significant difference ($p>0.05$) between pressure and the torsion torque applied between 6 FSU's and torsion, 6 DBU's and torsion, and

the FSU's compared with the DBU's and torsion. The mean pressures of the 6 specimens tested ranged from 0.62 MPa to 0.68 MPa for FSU's and 0.52 MPa to 0.61 MPa for DBU's (Table 2). A trend in the 6 FSU's and 6 DBU's towards a decrease in intradiscal pressure with an increase in torsion torque was observed (Figure 30). However, the results revealed no significant differences in pressure when torsion torque was increased among and between FSU's and DBU's. Additionally, the standard deviations were large, due to high variability of the human specimens (Figure 30). Upon inspection of Table 2, specimens UM05H007 and UJ04J002 revealed a decrease in their confirmation pressures at 0 Nm after the test was completed, when compared to their pressures at 0 Nm before the test started. This was probably due to an artifact during testing.

When analyzing data, it was observed that 2 specimens had much lower average pressures for any given torsion torque. The lower average pressures were most likely due to disc degeneration, based on results of research performed by McNally and Adams (Figures 26-29). Those 2 specimens were removed from the analysis to determine if there any significant changes of pressure with an increase in torsion torque could be observed with a sample of normal discs $n=4$ (Table 4). The pressures increased slightly and showed a trend towards a pressure decrease with an increase in torsion torque. However, there was still no significant difference in pressure among and between the 4 FSU's and DBU's ($p>0.05$) (Table 5). The standard deviations decreased, however, revealing less variability of the human specimens with an $n=4$ (Figure 31).

3.5 The Effect of Disc Height with Applied Torsion

One of the goals of the research performed was to determine if disc height changes, specifically an increase, could be correlated with applied torsion torque under a predetermined loading protocol. To determine any difference in disc height, the amount of axial displacement had to be calculated. However,

although the rate of creep decreased during the testing, it did not reach equilibrium. This was concluded by examining creep curves of the FSU and DBU during initial loading (Figures 32, 33 and 34) and examining creep curves of the FSU and DBU during initial loading and testing (Figures 35 and 36). Because of this, the contribution due to creep had to be removed to obtain the possible disc height change due to torsion torque only, and not due to creep and torsion torque.

To determine the contribution due to creep, the following steps were taken. Axial displacement versus time was graphed showing creep and any height differences that occurred (Figure 37). Then, any height differences were removed and a logarithmic trendline added (Figure 38) to predict the axial displacement due to creep only (Figure 39). The axial displacement with height changes and creep was subtracted from the axial displacement due to creep alone. Finally, axial displacement showing any occurring height differences without creep were exposed (Figure 40). This procedure was repeated for all 6 FSU and all 6 DBU specimens (Figures 41-84).

To determine if disc height changed with applied torsion torque, graphs of axial displacement, torsion torque, and pressure were created (Figures 85-96). There was no change in disc height observed with an increase in torsion torque.

There was an observed difference in disc height some time after each torsional change that could be directly explained by the insertion of the cannula. For example, the torsion torque changed and held its position while disc height remained constant. When the cannula was inserted with the needle, however, a disc height difference could be observed (Figures 85-96). In fact, a disc height increase occurred during each cannula insertion into each specimen. The mean height difference ranged from 0.13 mm to 0.16 mm for all specimens (FSU and DBU) when any torsion torques were applied (Figure 97, Table 6).

This led to the question of whether the height increase changed as torsion was increased or with the removal of posterior elements. There was no significant difference between differential disc height due to specific torsion

torques applied ($p > 0.05$) (Tables 6 and 7). Additionally, there was no significant difference between differential disc height and torsion torques among and between the FSU's and the DBU's ($p > 0.05$) (Tables 6 and 7).

3.6 The Correlation of Pressure and Disc Height with Torsion

The linear regression analysis of pressure versus torsion for the 6 FSU's and 6 DBU's revealed no correlation (Table 8). Those slopes were negative and very close to zero. The analysis of pressure versus torsion for the 4 FSU's and 4 DBU's also revealed no correlation (Table 8). Those slopes were negative and very close to zero. Finally, the analysis of height versus torsion for the 6 FSU's and 6 DBU's revealed no correlation (Table 8). Those slopes were negative and very close to zero. Therefore, it can be said that there is no correlation of pressure or disc height with different torsion torques.

Chapter Four: Discussion

4.1 Discussion of Results

To our knowledge, the effects of varying torsion torques on disc height and intradiscal pressure in human L1-L2 specimens with and without posterior elements under 600 N have not been previously studied. It was found that torsion torques of 2 Nm and less had no instantaneous effects on the disc, either in disc height increase or intradiscal pressure decrease. However, a disc height increase occurred with the insertion of a cannula. Such an increase has valuable implications because it demonstrated how to gain disc height in an intervertebral disc (IVD). A method to increase disc height could lead to a low cost, minimally invasive technique to minimize chronic low back pain for millions of people.

The current research did not find a significant increase in disc height or decrease in intradiscal pressure of the human L1-L2 disc space. However, if other human functional spine units (FSU's) demonstrate a disc height increase under different parameters, then clinical relevance could be applied in approaches such as therapies, treatments, or surgeries that reflect the results. Other human FSU specimens could reveal different results because the facet joints of the human lumbar spine are oriented differently as one proceeds caudally down the spine. For example, the L1-L2 facets joints are oriented closer to the mid-sagittal plane at about 26-34°, while the L5-S1 facet joints are oriented farther from the mid-sagittal plane at about 40-56°. ²² The facet joints in between those act as transitions, and are therefore oriented accordingly. The facet joints of the lower vertebral bodies may 'ride up' on each other during torsional rotations and it may be possible to obtain a decrease in intradiscal pressure and an increase in disc height in those motion segments. Since low back pain (LBP)

is prevalent in the lower motion segments (ie: L3-L4, L4-L5 and L5-S1), it could be very important to determine the validity of this hypothesis.

There was no disc height increase due to torsion observed in this study, however, there was a disc height increase seen due to the insertion of the cannula. The implications are important regarding future work because more research could lead to the development of a biocompatible material of a specific size to be inserted into a degenerated disc to regain disc height. The height gain would have an immediate, pain-reducing effect through the decrease of contact forces on facet joints, the increase in foraminal space, and the normalization of pressure distribution in the disc.³⁷ In addition, it can be inferred that the height gain would enhance avascular nutrition and thus counteract degenerative changes.³⁷

In order for the pressure probe to record compressive pressure consistently, the pressure must act evenly on the probe membrane, requiring the surrounding medium to be capable of conforming to its surface.²⁴ Because plateaus or peaks can be seen in all graphs, it can be inferred that the pressure probe accurately recorded the pressures taken and that there was enough mobile proteoglycans-water gel combination in the IVD's to be accurately measured. The tests revealed that the pressure measurements were reproducible and did not significantly alter the tissues being studied.

4.2 Limitations

4.2.a Sample Size and Variability

The small sample size (n=6) and variability were limitations of this research. The small sample size led to an underpowered study both with the analysis using 6 specimens (Power=65%) and with the analysis using 4 specimens (Power=50%). The high variability of the specimens including age range and disc condition, led to high standard deviations.

4.2.b Testing

Torsion torques of less than 2 Nm were used in order to keep the forces within physiologic loading ranges. However, the range of motion was up to 3°, which is less than the maximum ranges of motion reported in Panjabi and White. Loading should not damage the motion segment, but could incorporate the higher end of the range (ie: 6°).³⁹ It could be possible that higher torsion torques could reveal a decrease in intradiscal pressure and an increase in disc height.

Only two degrees of freedom were used in the current research, because of the degradation and dehydration issues associated with the lengthening of the testing time. However, other degrees of freedom including flexion-extension and lateral bending could demonstrate a change in intradiscal pressure and disc height.

One lumbar motion segment (L1-L2) was used to perform these tests. This was due specifically to specimen availability. Although the L1-L2 motion segment generated useful results, the motion segments in the lower lumbar spine (ie: L4-L5 and L5-S1) are highly associated with low back pain (LBP). Therefore, determining the results of increased torsion torques on intradiscal pressure and disc height in other motion segments would be important.

Chapter Five: Future Work

5.1 Research

5.1.a Sample Size and Variability

Although there was some variety of the degree of degeneration in the discs used in this research, a future study could include a much larger sample size of nondegenerated discs and severely degenerated discs to compare age to degeneration. Although the testing performed revealed important results regarding disc height and intradiscal pressure changes with different applied torsion torques, it is hard to make generalizations with only 6 specimens. Additionally, the dynamic properties of the spine may be lost with age and degeneration. Therefore, future work would include testing a larger sample size of nondegenerated and degenerated FSU's and DBU's using the same testing parameters.

5.1.b Testing

The current research also revealed that different applied torsion torques less than 2 Nm do not significantly increase disc heights nor decrease intradiscal pressures. Although the pressures tend to decrease with increased applied torsion torques, there was no significant change in pressure. Even though this finding is very important, a question arises as to whether applied torsion torques greater than 2 Nm would have similar or opposite effects under the same loading conditions. Since 2 Nm is a very small applied torque, it would be useful to determine what result higher torsion torques yield, under the same loading conditions. Future steps would include testing the specimens up to a specimen-specific physiologic applied torsion torque, under the same loading conditions. In

addition to testing specimens under larger applied torsion torques as described above, it would be beneficial to test the same torsion torques at different loading rates. Different loading rates of torsion torque could show a different outcome because loading rates would change the stiffness of the disc. As a result, this may have a significant effect on disc height and intradiscal pressure.

The current research focused on determining disc height and intradiscal pressure changes in only the torsion degree of freedom with axial compression. Important future work would expand the testing of torsion torques on disc heights and intradiscal pressures to include other degrees of freedom such as flexion, extension, left bending and right bending under similar loading conditions. The effects of different torques and angles in other degrees of freedom could reveal important effects that various torques have on disc height and intradiscal pressures. The likelihood of specimen degradation occurring under repeated loading prevented the testing of all combinations on each motion segment in this research. Although testing in all 6 degrees of freedom would present a considerable problem with regard to degradation, an improvement in the testing environment could help alleviate this problem. Designing and building a tank capable of testing specimens in a simulated ideal physiologic testing environment (37°C saline water) could help to minimize the occurrence of degradation, while being able to determine disc height and intradiscal pressure changes in specimens in all ranges of motion. This would necessitate the design of a new fixture system, but could be worth the investment.

Another area of significant future work includes studying disc height and intradiscal pressure changes among other functional spine units in the lumbar spine. Although the availability of specimens limited this research to testing only the L1-L2 motion segments, it would be valuable to study other segments for a significant reason. Since the facet joints of the human lumbar spine are oriented differently as you proceed caudally down the spine, it could be useful to determine if the orientation of the facet joints play a role in any disc height or intradiscal pressure changes with increased torsion torques. It is hypothesized

that while there would be no change seen in the rostral motion segments with transitional facet joint orientations (ie: L2-L3 and L3-L4), the lower motion segments (ie: L4-L5 and L5-S1) may reveal a disc height gain or an intradiscal pressure decrease. If there was an observed height change of the lower segments and not the upper segments, it could be explained by a phenomenon of the facet joints riding up on each other that facilitates the changes. This has clinical significance because pain reducing therapies, including torsion torque, could be incorporated into treatment for people with low back pain.

5.2 Applications

The current research demonstrated that while disc height increases were not observed with changes in torsion torque, disc height increases were seen with the insertion of the cannula. This is a very important finding as this shows how to gain disc height in a degenerated IVD. In fact, if a cannula of a specific size can increase disc height, then it can be hypothesized that the addition of specific materials of a certain size will cause an increase in disc height as well. For example, material of a specific diameter and length could be inserted to gain disc height. The advantages surrounding this idea include an appealing minimally invasive technique as well as a lower cost product and surgical procedure. Obviously a great deal of future work surrounds this idea on the order of determining types, shapes and sizes of materials, interactions with biological tissue, migration, and patient candidacy, to name a few, but it opens the doors for new research.

References

1. Adams, M., Bogduk, N., Burton, K., Dolan, P. Biomechanics of back pain. Churchill Livingstone. 2002.
2. Adams, M.A., McMillan, D.W., Green, T.P., Dolan, P. Sustained loading generates stress concentrations in lumbar intervertebral discs. *Spine*. 1996; 21: 434-438.
3. Adams, M.A., McNally, D.S., Dolan, P. "Stress" distribution inside intervertebral discs. *J Bone Joint Surg*. 1996; 78: 965-972.
4. Ashman, R.B. Disc anatomy and biomechanics. *Spine*. 1989; 3: 13-26.
5. Buckwalter, J.A. Spine Update: Aging and Degeneration of the Human Intervertebral Disc. *Spine*. 1995; 20: 1307-1314.
6. Bushell, G.R., Ghosh, P., Taylor, T.F., Akeson, W.H. Proteoglycan chemistry of the intervertebral discs. *Clin Orthop*. 1977; 115-123.
7. Crock, H.V., Yoshizawa, H. The blood supply of the lumbar vertebral column. *Clin Orthop*. 1976; 6-21.
8. Dhillon, Nripendra, Bass, Elisa, Lotz, Jeffrey. Effect of frozen storage on the creep behavior of human intervertebral discs. *Spine*. 2000.; 26: 883-888.
9. Ekstrom, L., Holm, S., Holm, A.K., Hansson, T. *In vivo* porcine intradiscal pressure as a function of external loading. *J Spinal Disord Tech*. 2004; 17: 312-316.

10. Evans, W., Jobe, W., Seibert, C. A cross-sectional prevalence study of lumbar disc degeneration in a working population. *Spine*. 1989; 14: 60-64.
11. Fung, Y.C. *Biomechanics: Mechanical Properties of Living Tissues*. New York, Springer-Verlag. 1993.
12. Hayes, A.J., Benjamin, M., Ralphs, J.R. Intracellular matrix in development of the intervertebral disc. *Matrix Biology*. 2001; 20: 107-121.
13. Horst, M., Brinckmann, P. Measurement of the distribution of axial stress on the end-plate of the vertebral body. *Spine*. 1981; 6: 217-232.
14. Hukins, D.W.L., Meakin, J.R. Relationship between structure and mechanical function of the tissues of the intervertebral joint. *Amer Zool*. 2000; 40: 42-52.
15. Humzah, M.D., Soames, R.W. Human intervertebral disc: structure and function. *Anat Rec*. 1988; 220: 337-356.
16. Iatridis, J.C., MacLean, J.J., Ryan, D.A. Mechanical damage to the intervertebral disc annulus fibrosus subjected to tensile loading. *J Biomech*. 2004; 38: 557-565.
17. Janevie, J., Ashton-Miller, J., Schultz, A. Large compressive preloads decrease lumbar motion flexibility. *J Orthop Res*. 1991; 9: 228-236.
18. Johnstone, B. Urban, J.P.G., Roberts, S., Menage, J. The fluid content of the human intervertebral disc: comparison between fluid content and swelling pressure profiles of discs removed at surgery and those taken postmortem. *Spine*. 1992; 17: 412-416.
19. Lee, S.H., Derby, R., Chen, Y., Seo, K.S., Kim, M.J. In vitro measurement of pressure in intervertebral discs and annulus fibrosus with and without annular tears during discography. *Spine J*. 2004; 4: 614-618.

20. Lu, Y.M., Hutton, W.C., Gharpuray, V.M. Can variations in intervertebral disc height affect the mechanical function of the disc? *Spine*. 1996; 21: 2208-2216.
21. Marieb, E.N., Mallatt, J. *Human Anatomy*, Third Edition. Benjamin Cummings. 2001. 160-184.
22. Masharawi, Y., Rothschild, B., Dar, G., Peleg, S., Robinson, D., Been, E., Hershkovitz, I. Facet orientation in the thoracolumbar spine. *Spine*. 2004; 29: 1755-1763.
23. McMillan, D., McNally, D.S., Garbutt, G. Stress distributions inside intervertebral discs: the validity of experimental "stress profilometry". *Proc Mech Inst Eng*. 1996; 210: 81-87.
24. McNally, D.S., Adams, M.A. Internal intervertebral disc mechanics as revealed by stress profilometry. *Spine*. 1992; 17: 66-73.
25. Mercer, S., Bogduk, N. The ligaments and annulus fibrosus of human adult cervical intervertebral discs. *Spine*. 1999; 24: 619-628.
26. Mimura, M., Panjabi, M.M., Oxland, T.R., Crisco, J.J., Yamamoto, I., Vasavada, A. Disc degeneration affects the multidirectional flexibility of the lumbar spine. *Spine*. 1994; 19: 1371-1380.
27. Nachemson, A. Disc pressure measurements. *Spine*. 1981; 6:93-97.
28. Niosi, C.A., Oxland, T.R. Degenerative mechanics of the lumbar spine. *Spine J*. 2004; 4: 202S-208S.
29. Nordin, M., Frankel, V.H. *Basic Biomechanics of the Musculoskeletal System*, Third Edition. Philadelphia, PA, Lippincott Williams and Wilkins. 2001. 10-14, 257-260, 293-295.

30. Park, C., Kim, Y.J., Lee, C.S., An, K., Shin, H.J., Chang, H., Kim, C.H., Shin, J.W. An *in vitro* animal study of the biomechanical responses of annulus fibrosus with aging. *Spine*. 2005; 30: E259-E265.
31. Panjabi, M.M., Goel, V., Oxland, T., Takata, K., Duranceau, J., Krag, M., Price, M. Human lumbar vertebrae: quantitative three-dimensional anatomy. *Spine*. 1992; 17: 299-306.
32. Polga, D.J., Beaubien, B.P., Kallemeier, P.M., Schellhas, K.P., Lew, W.D., Buttermann, G.R., Wood, K.B. Measurement of *in vivo* intradiscal pressure in healthy thoracic intervertebral discs. *Spine*. 2004; 29: 1320-1324.
33. Sato, K., Kikuchi, S., Yonezawa, T. *In vivo* intradiscal pressure measurements in healthy individuals and in patients with ongoing back problems. *Spine*. 1999; 24: 2468-2474.
34. Selard, E., Shirazi-Adl, A., Urban, J.P.G. Finite element study of nutrient diffusion in the human intervertebral disc. *Spine*. 2003; 28: 1945-1953.
35. Shirazi-Adl, S.A., Shrivastava, S.C., Ahmed, A.M. Stress analysis of the lumbar disc-body unit in compression: a three-dimensional nonlinear finite element study. *Spine*. 1984; 9: 120-133.
36. Steffen, T., Baramki, H.G., Rubin, R., Antoniou, J., Aebi, M. Lumbar intradiscal pressure measured in the anterior and posterolateral annular regions during asymmetrical loading. *Clin Biomech*. 1998; 13: 495-505.
37. van Deursen, D.L., Snijders, C.J., Kingma, I., van Dieen, J.H. *In vitro* torsion-induced stress distribution changes in porcine intervertebral discs. *Spine*. 2001; 26: 282-286.
38. Wang, J.L., Parnianpour, M., Shirazi-Adl, A., Engin, A.E. The dynamic response of L₂/L₃ motion segment in cyclic axial compressive loading. *Clin Biomech*. 1998; 13: S16-S25.

39. White, A.A., Panjabi, M.M. *Clinical Biomechanics of the Spine*, Second Edition. Philadelphia, PA, Lippincott Williams and Wilkins. 1990.
40. Wilke, H., Claes, L., Schmitt, H. A universal spine tester for in vitro experiments with muscle force simulation. *Eur Spine J.* 1994; 3: 91-97.
41. Wilke, H.J., Neef, P., Caimi, M., Hoogland, T., Claes, L.E. New *in vivo* measurements of pressures in the intervertebral disc in daily life. *Spine.* 1999; 24: 755-762.
42. Wilke, H.J., Wolf, S., Claes, L.E., Arand, M., Wiesend, A. Influence of varying muscle forces on lumbar intradiscal pressure: an *in vitro* study. *J. Biomechanics.* 1996; 29: 549-555.
43. Yingling, V.R., Callaghan, J.P., McGill, S.M. The porcine cervical spine as a model of the human lumbar spine: an anatomical, geometric, and functional comparison. *J Spinal Disord.* 1999; 12: 415-423.

Appendices

Appendix A – Tables

Table 1 - Cadaveric Specimen Record

<u>Gender</u>	<u>Age (yr)</u>	<u>Level</u>
F	38	L1-L2
F	49	L1-L2
M	43	L1-L2
M	52	L1-L2
F	65	L1-L2
M	56	L1-L2
Avg age: 50.5 yrs		

Appendix A – (Continued)

Table 2 - Mean Pressures of 6 FSU and 6 DBU Specimens (n=6)

Avg Pressure (MPa) FSU
n=6

	<u>0 Torque</u> <u>(Nm)</u>	<u>0.5</u> <u>Torque</u> <u>(Nm)</u>	<u>1.0 Torque</u> <u>(Nm)</u>	<u>2.0 Torque</u> <u>(Nm)</u>	<u>0 conf Torque</u> <u>(Nm)</u>
Pressure	MPa	MPa	MPa	MPa	MPa
UT04K009 FSU Test 1	0.77	0.78	0.77	0.77	0.77
UM05H007 FSU Test 1	0.44	0.36	0.38	0.32	0.36
UJ04L015 FSU Test 1	0.90	0.85	0.86	0.86	0.84
UJ04J002 FSU Test 1	0.91	0.74	0.73	0.72	0.72
UF05H007 FSU Test 1	0.75	0.74	0.73	0.72	0.72
UF05B003 FSU Test 1	0.32	0.33	0.27	0.35	0.31
Mean FSU	0.68	0.63	0.62	0.62	0.62
SD FSU	0.24	0.23	0.24	0.23	0.23

Avg Pressure (MPa) DBU
n=6

	<u>0 Torque</u> <u>(Nm)</u>	<u>0.5</u> <u>Torque</u> <u>(Nm)</u>	<u>1.0 Torque</u> <u>(Nm)</u>	<u>2.0 Torque</u> <u>(Nm)</u>	<u>0 conf Torque</u> <u>(Nm)</u>
Pressure	MPa	MPa	MPa	MPa	MPa
UT04K009 DBU Test 2	0.71	0.71	0.71	0.70	0.69
UM05H007 DBU Test 2	0.46	0.33	0.24	0.44	0.33
UJ04L015 DBU Test 2	0.84	0.82	0.79	0.76	0.61
UJ04J002 DBU Test 2	0.73	0.72	0.70	0.69	0.68
UF05H007 DBU Test 2	0.72	0.71	0.70	0.70	0.70
UF05B003 DBU Test 2	0.19	0.29	0.11	0.25	0.12
Mean DBU	0.61	0.60	0.54	0.59	0.52
SD DBU	0.24	0.23	0.29	0.20	0.24

Appendix A – (Continued)

Table 3 - Compiled Pressure Versus Torque ANOVAS for 6 FSU and 6 DBU Specimens (n=6)

FSU Pressure vs. Torque ANOVAS

		<u>P-value</u>	
0 Nm FSU	0.5 Nm FSU	0.73	>0.05
0 Nm FSU	1.0 Nm FSU	0.70	>0.05
0 Nm FSU	2.0 Nm FSU	0.67	>0.05
0.5 Nm FSU	1.0 Nm FSU	0.95	>0.05
0.5 Nm FSU	2.0 Nm FSU	0.93	>0.05
1.0 Nm FSU	2.0 Nm FSU	0.98	>0.05

DBU Pressure vs. Torque ANOVAS

		<u>P-value</u>	
0 Nm DBU	0.5 Nm DBU	0.92	>0.05
0 Nm DBU	1.0 Nm DBU	0.66	>0.05
0 Nm DBU	2.0 Nm DBU	0.89	>0.05
0.5 Nm DBU	1.0 Nm DBU	0.72	>0.05
0.5 Nm DBU	2.0 Nm DBU	0.97	>0.05
1.0 Nm DBU	2.0 Nm DBU	0.73	>0.05

FSU and DBU Pressure vs. Torque ANOVAS

		<u>P-value</u>	
0 Nm FSU	0 Nm DBU	0.62	>0.05
0.5 Nm FSU	0.5 Nm DBU	0.78	>0.05
1.0 Nm FSU	1.0 Nm DBU	0.59	>0.05
2.0 Nm FSU	2.0 Nm DBU	0.82	>0.05

Appendix A – (Continued)

Table 4 - Mean Pressures of 4 FSU and 4 DBU Specimens (n=4)

*Avg Pressure (MPa) FSU
n=4*

	<u>0 Torque (Nm)</u>	<u>0.5 Torque (Nm)</u>	<u>1.0 Torque (Nm)</u>	<u>2.0 Torque (Nm)</u>
Pressure	MPa	MPa	MPa	MPa
UT04K009 FSU Test 1	0.77	0.78	0.77	0.77
UJ04L015 FSU Test 1	0.90	0.85	0.86	0.86
UJ04J002 FSU Test 1	0.91	0.74	0.73	0.72
UF05H007 FSU Test 1	0.75	0.74	0.73	0.72
Mean FSU	0.83	0.78	0.77	0.76
SD FSU	0.08	0.05	0.06	0.06

*Avg Pressure (MPa) DBU
n=4*

	<u>0 Torque (Nm)</u>	<u>0.5 Torque (Nm)</u>	<u>1.0 Torque (Nm)</u>	<u>2.0 Torque (Nm)</u>
Pressures	MPa	MPa	MPa	MPa
UT04K009 DBU Test 2	0.71	0.71	0.71	0.70
UJ04L015 DBU Test 2	0.84	0.82	0.79	0.76
UJ04J002 DBU Test 2	0.73	0.72	0.70	0.69
UF05H007 DBU Test 2	0.72	0.71	0.70	0.70
Mean DBU	0.75	0.74	0.72	0.72
SD DBU	0.06	0.05	0.04	0.03

Appendix A – (Continued)

Table 5 - Compiled Pressure Versus Torque ANOVAS for 4 FSU and 4 DBU Specimens (n=4)

FSU Pressure vs. Torque ANOVAS

		<u>P-value</u>	
0 Nm FSU	0.5 Nm FSU	0.31	>0.05
0 Nm FSU	1.0 Nm FSU	0.32	>0.05
0 Nm FSU	2.0 Nm FSU	0.25	>0.05
0.5 Nm FSU	1.0 Nm FSU	0.97	>0.05
0.5 Nm FSU	2.0 Nm FSU	0.78	>0.05
1.0 Nm FSU	2.0 Nm FSU	0.83	>0.05

DBU Pressure vs. Torque ANOVAS

		<u>P-value</u>	
0 Nm DBU	0.5 Nm DBU	0.78	>0.05
0 Nm DBU	1.0 Nm DBU	0.50	>0.05
0 Nm DBU	2.0 Nm DBU	0.35	>0.05
0.5 Nm DBU	1.0 Nm DBU	0.68	>0.05
0.5 Nm DBU	2.0 Nm DBU	0.49	>0.05
1.0 Nm DBU	2.0 Nm DBU	0.77	>0.05

FSU and DBU Pressure vs. Torque ANOVAS

		<u>P-value</u>	
0 Nm FSU	0 Nm DBU	0.17	>0.05
0.5 Nm FSU	0.5 Nm DBU	0.35	>0.05
1.0 Nm FSU	1.0 Nm DBU	0.23	>0.05
2.0 Nm FSU	2.0 Nm DBU	0.23	>0.05

Appendix A – (Continued)

Table 6 - Mean Height Differences of all 6 FSU and 6 DBU Specimens

Avg Height Difference (mm) FSU

	<u>0 Torque (Nm)</u>	<u>0.5 Torque (Nm)</u>	<u>1.0 Torque (Nm)</u>	<u>2.0 Torque (Nm)</u>
Height Differences	mm	mm	mm	mm
UT04K009 FSU Test 1	0.18	0.14	0.14	0.14
UM05H007 FSU Test 1	0.12	0.09	0.12	0.11
UJ04L015 FSU Test 1	0.15	0.14	0.11	0.12
UJ04J002 FSU Test 1	0.21	0.15	0.15	0.17
UF05H007 FSU Test 1	0.18	0.16	0.20	0.14
UF05B003 FSU Test 1	0.10	0.09	0.05	0.11
Mean FSU	0.16	0.13	0.13	0.13
SD FSU	0.04	0.03	0.05	0.02

Avg Height Difference (mm) DBU

	<u>0 Torque (Nm)</u>	<u>0.5 Torque (Nm)</u>	<u>1.0 Torque (Nm)</u>	<u>2.0 Torque (Nm)</u>
Height Differences	mm	mm	mm	mm
UT04K009 DBU Test 2	0.17	0.14	0.12	0.12
UM05H007 DBU Test 2	0.14	0.13	0.13	0.17
UJ04L015 DBU Test 2	0.16	0.13	0.13	0.12
UJ04J002 DBU Test 2	0.13	0.17	0.16	0.15
UF05H007 DBU Test 2	0.18	0.16	0.12	0.14
UF05B003 DBU Test 2	0.12	0.12	0.06	0.07
Mean DBU	0.15	0.14	0.12	0.13
SD DBU	0.02	0.02	0.03	0.03

Appendix A – (Continued)

Table 7 - Compiled Height Versus Torque ANOVAS for 6 FSU and 6 DBU Specimens

FSU Heights vs. Torque ANOVAS

		<u>P-value</u>	
0 Nm FSU	0.5 Nm FSU	0.18	>0.05
0 Nm FSU	1.0 Nm FSU	0.28	>0.05
0 Nm FSU	2.0 Nm FSU	0.21	>0.05
0.5 Nm FSU	1.0 Nm FSU	0.97	>0.05
0.5 Nm FSU	2.0 Nm FSU	0.82	>0.05
1.0 Nm FSU	2.0 Nm FSU	0.84	>0.05

DBU Heights vs. Torque ANOVAS

		<u>P-value</u>	
0 Nm DBU	0.5 Nm DBU	0.77	>0.05
0 Nm DBU	1.0 Nm DBU	0.14	>0.05
0 Nm DBU	2.0 Nm DBU	0.32	>0.05
0.5 Nm DBU	1.0 Nm DBU	0.18	>0.05
0.5 Nm DBU	2.0 Nm DBU	0.42	>0.05
1.0 Nm DBU	2.0 Nm DBU	0.65	>0.05

FSU and DBU Heights vs. Torque ANOVAS

		<u>P-value</u>	
0 Nm FSU	0 Nm DBU	0.63	>0.05
0.5 Nm FSU	0.5 Nm DBU	0.32	>0.05
1.0 Nm FSU	1.0 Nm DBU	0.83	>0.05
2.0 Nm FSU	2.0 Nm DBU	0.93	>0.05

Appendix A – (Continued)

Table 8 - Linear Regression Analysis

Linear Regression Analysis

<i>Pressure vs. Torque n=6</i>	<i>Slope</i>
FSU	-0.03
DBU	-0.01
<hr/>	
<i>Pressure vs. Torque n=4</i>	<i>Slope</i>
FSU	-0.03
DBU	-0.02
<hr/>	
<i>Height vs. Torque n=6</i>	<i>Slope</i>
FSU	-0.01
DBU	-0.01

Appendix B – Figures

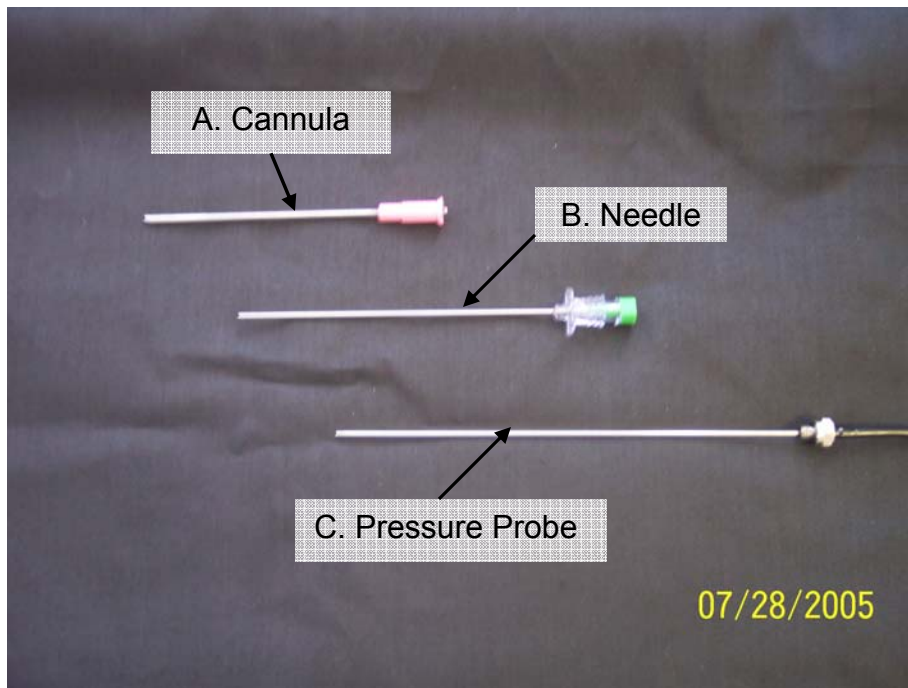


Figure 1 - A. Cannula, B. Needle and C. Pressure Probe

Appendix B – (Continued)

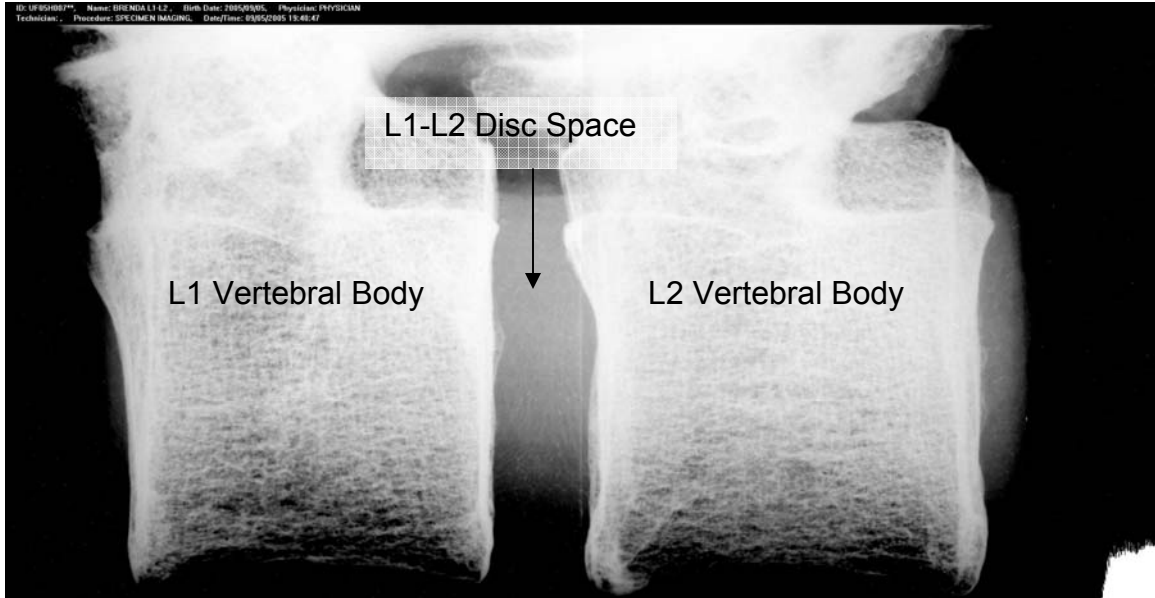


Figure 2 - X-ray of FSU UF05H007

Appendix B – (Continued)



Figure 3 - MRI of Lumbar Spine UT04K009

Appendix B – (Continued)



Figure 4 - MRI of Lumbar Spine UF05B003

Appendix B – (Continued)

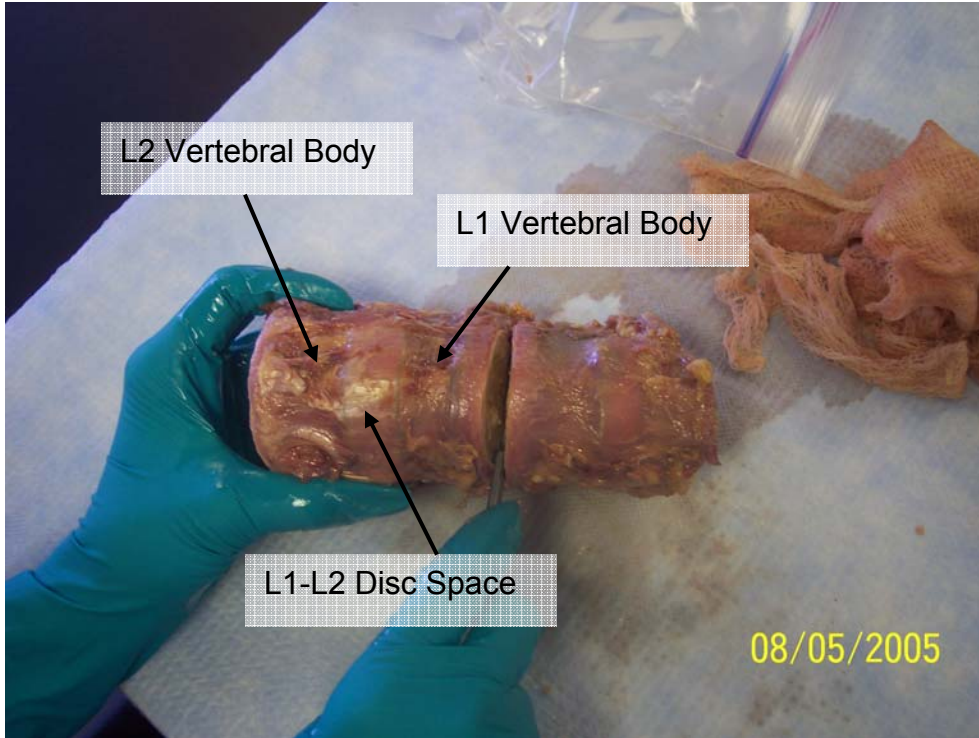


Figure 5 - Disarticulation of a Spine into an FSU (Functional Spine Unit)

Appendix B – (Continued)

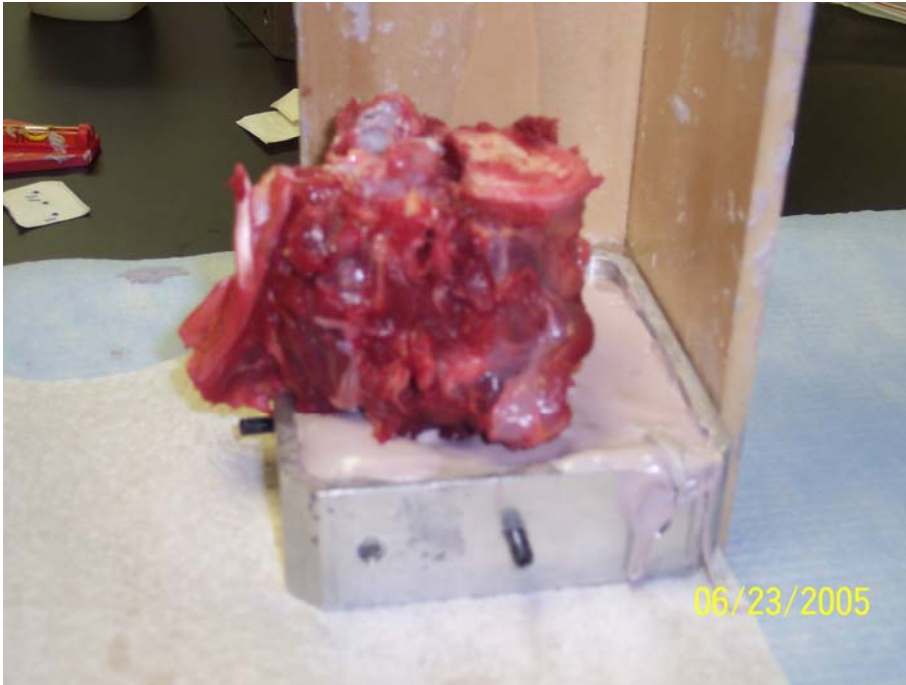


Figure 6 - Potted L2 Vertebral Body

Appendix B – (Continued)



Figure 7 - Potted L1 Vertebral Body

Appendix B – (Continued)

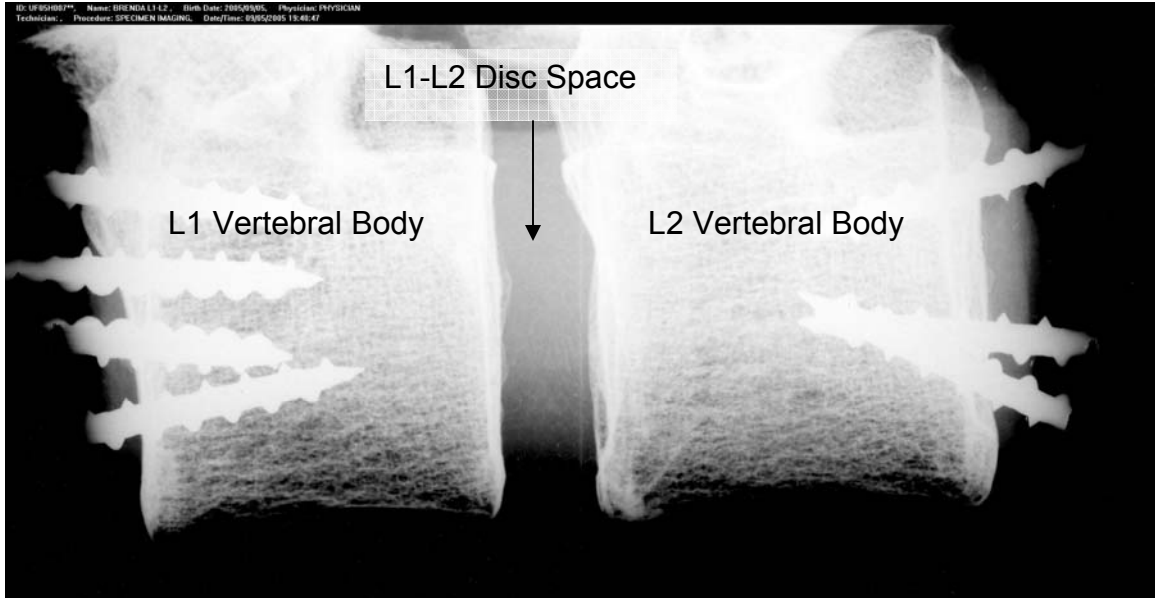


Figure 8 - X-ray of FSU UF05H007 with Screws

Appendix B – (Continued)

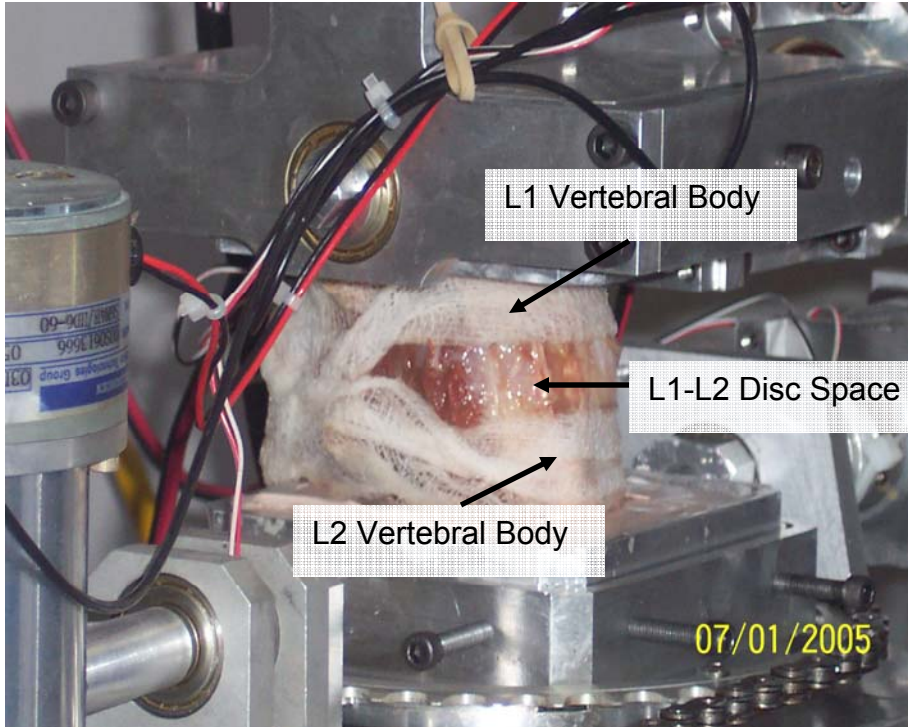


Figure 9 - Axial Compression of an FSU in the MTS Machine

Appendix B – (Continued)

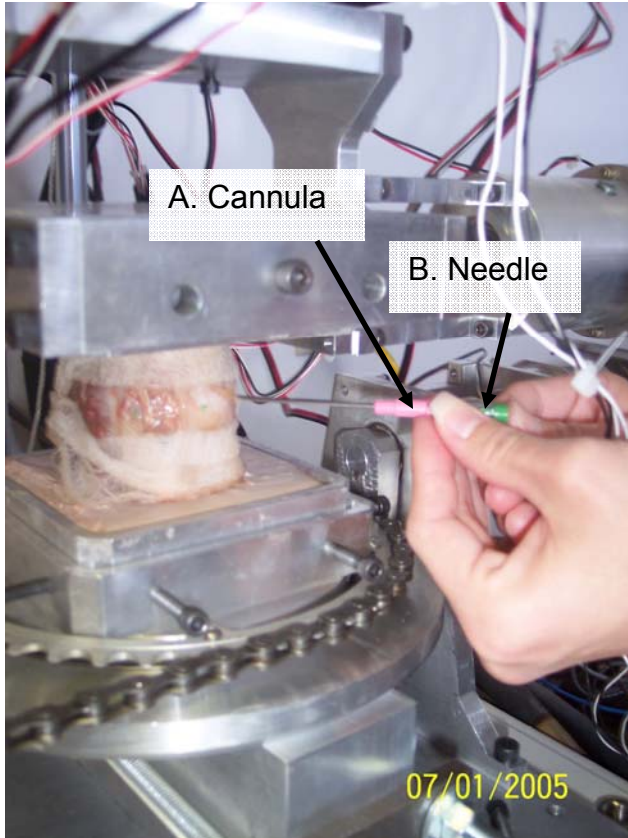


Figure 10 - Insertion of the A. Cannula and B. Needle into an FSU

Appendix B – (Continued)

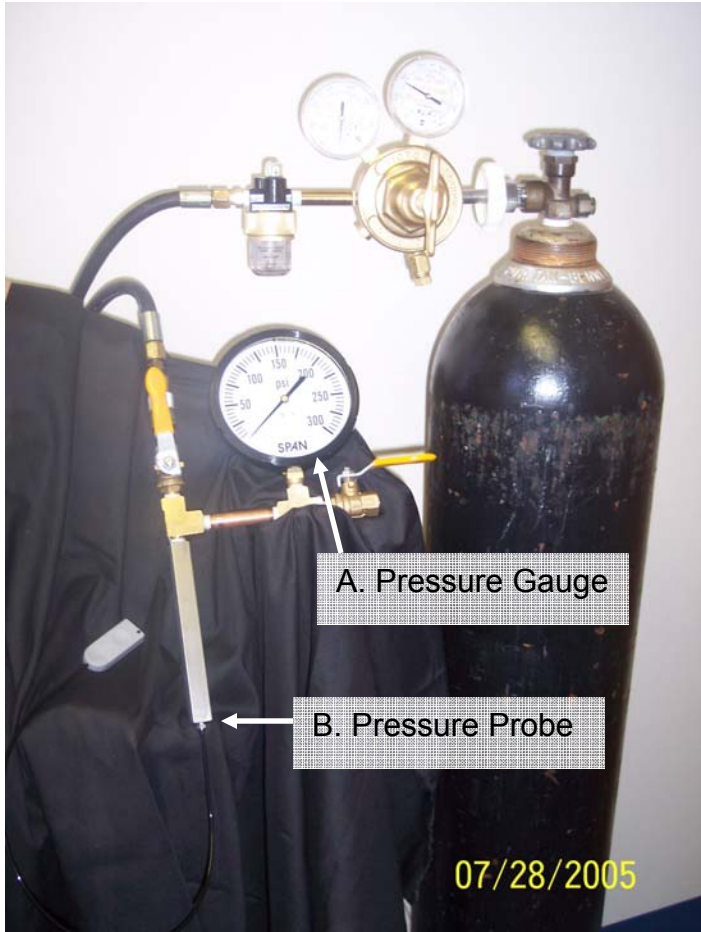


Figure 11 - A. Pressure Gauge and B. Pressure Probe

Appendix B – (Continued)

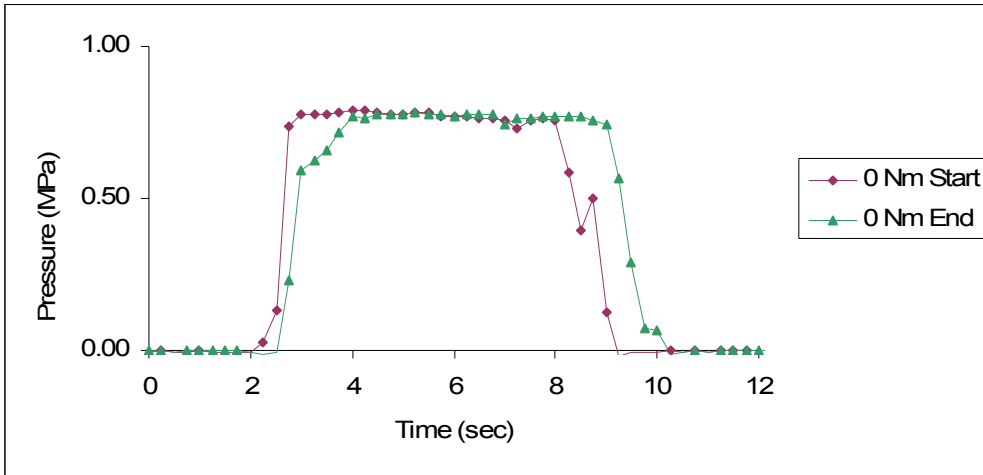


Figure 12 - Pressure of FSU UT04K009. Taken at 0 Nm Torque at the Start and End of the Testing Protocol

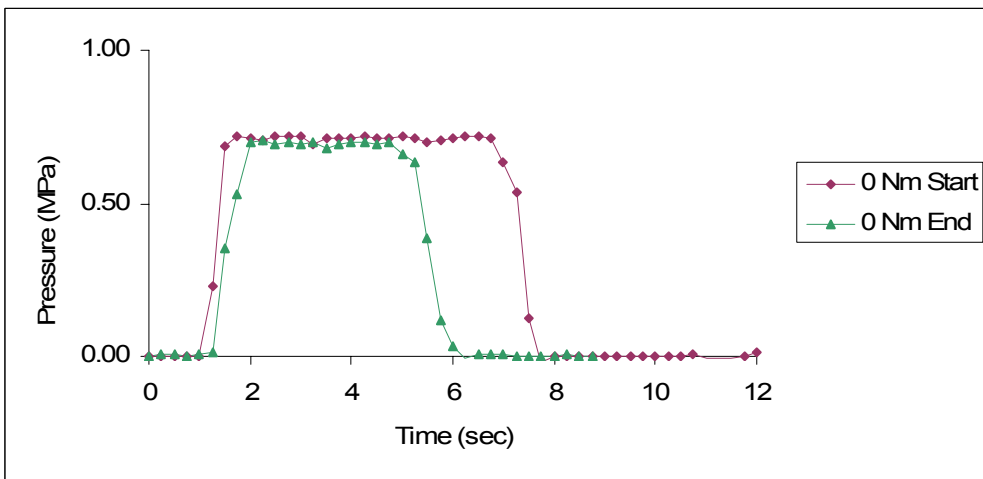


Figure 13 - Pressure of DBU UT04K009. Taken at 0 Nm Torque at the Start and End of the Testing Protocol

Appendix B – (Continued)

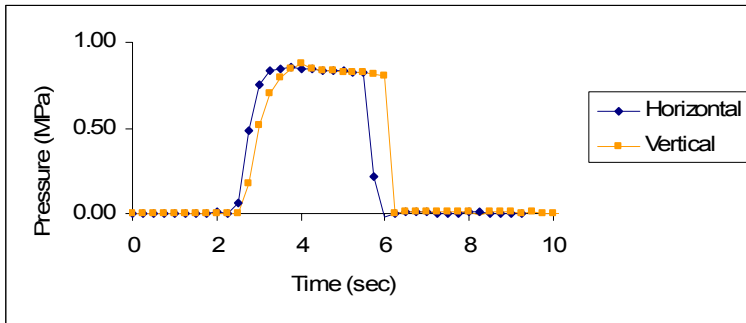


Figure 14 - Probe Orientations of DBU UJ04L015 at 0 Nm Torsion Torque

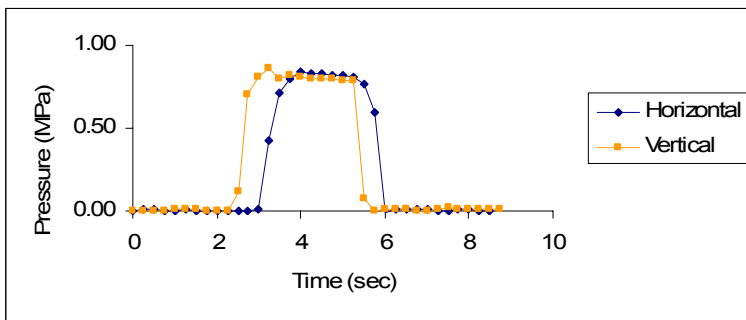


Figure 15 - Probe Orientations of DBU UJ04L015 at 0.5 Nm Torsion Torque

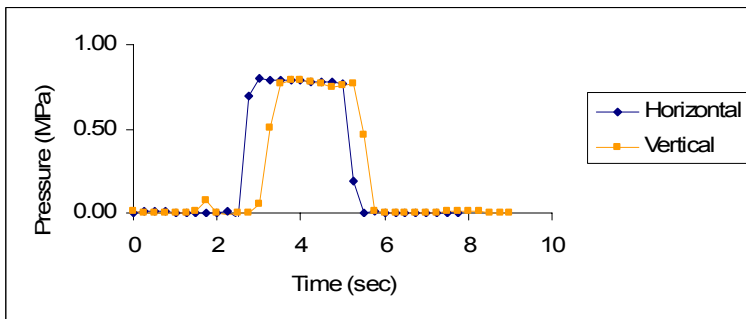


Figure 16 - Probe Orientations of DBU UJ04L015 at 1.0 Nm Torsion Torque

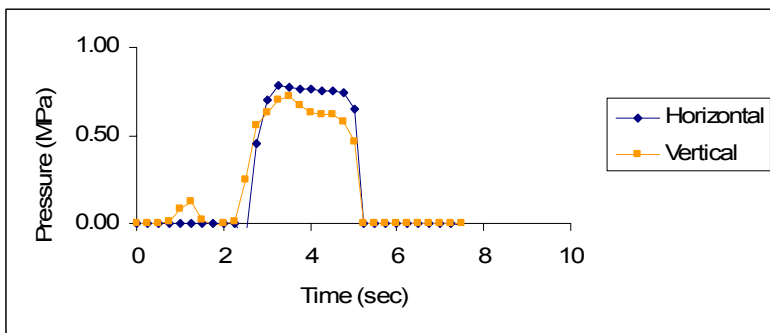


Figure 17 - Probe Orientations of DBU UJ04L015 at 2.0 Nm Torsion Torque

Appendix B – (Continued)

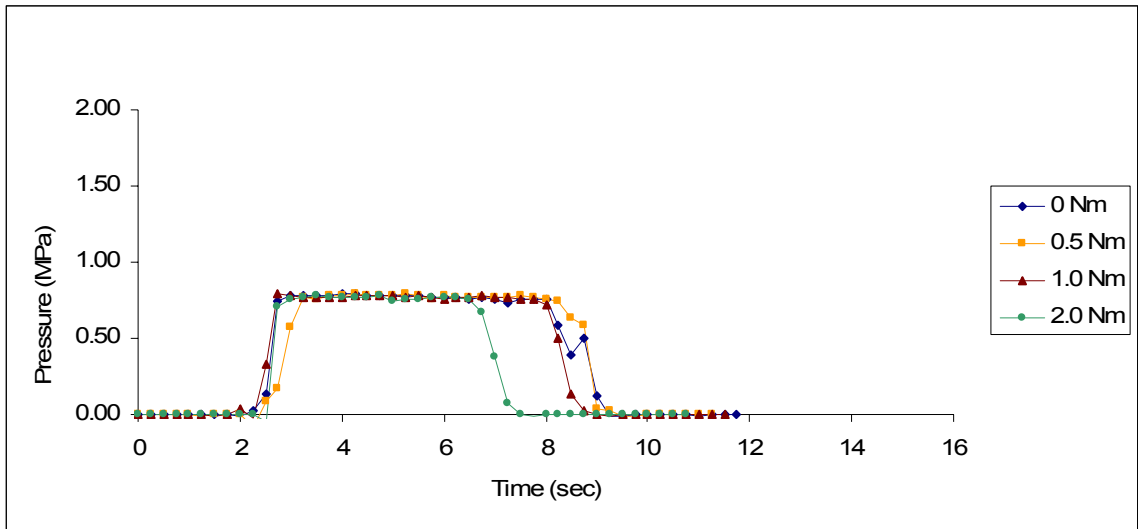


Figure 18 - Pressure of FSU UT04K009 at Different Torques

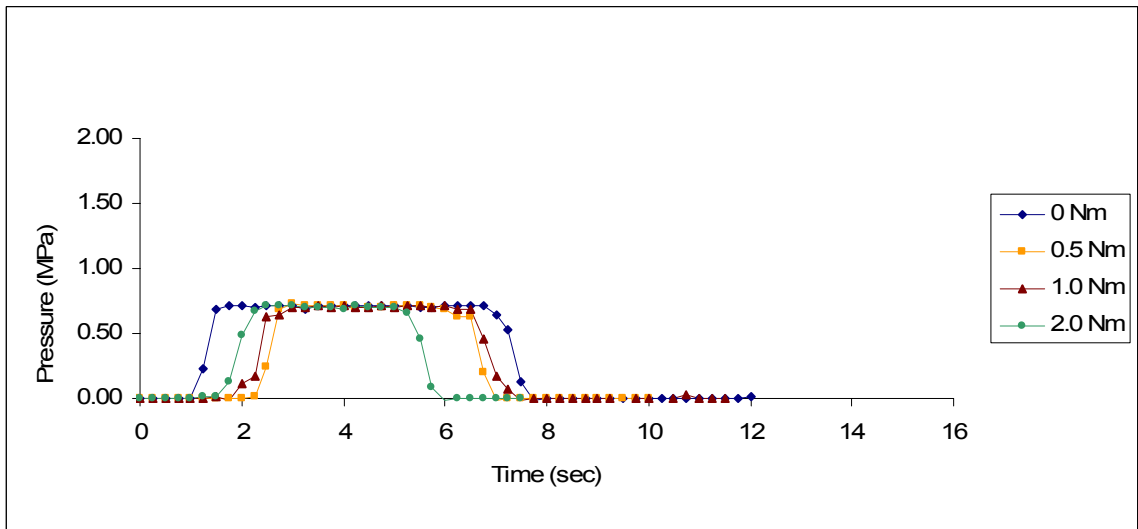


Figure 19 - Pressure of DBU UT04K009 at Different Torques

Appendix B – (Continued)

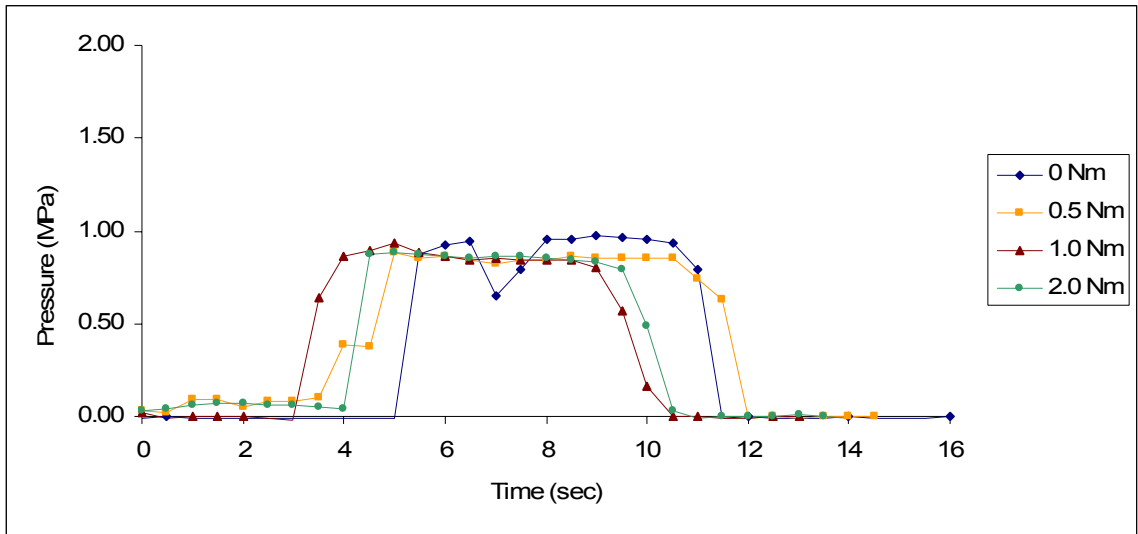


Figure 20 - Pressure of FSU UJ04L015 at Different Torques

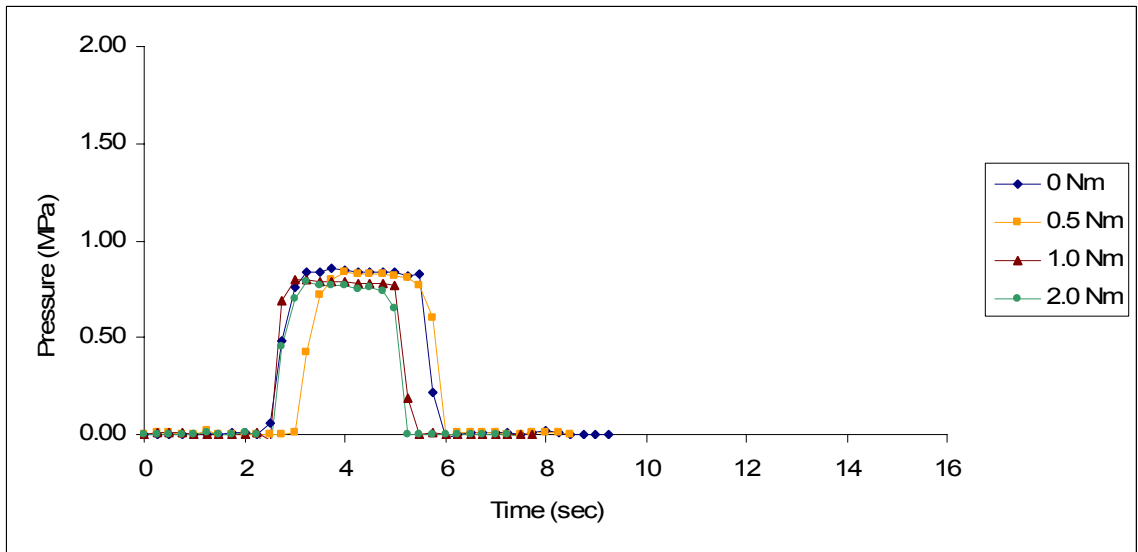


Figure 21 - Pressure of DBU UJ04L015 at Different Torques

Appendix B – (Continued)

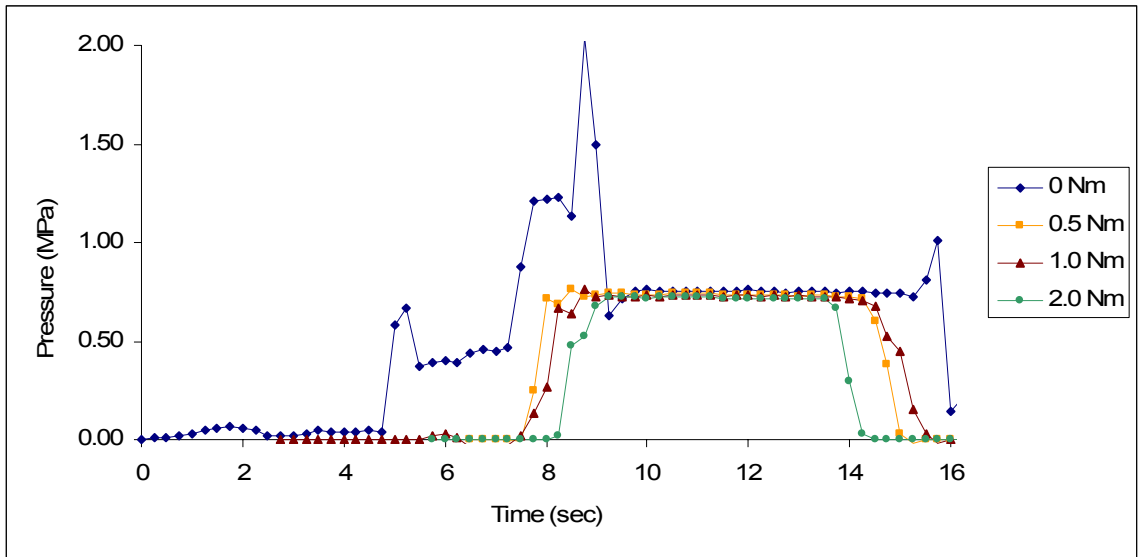


Figure 22 - Pressure of FSU UJ04J002 at Different Torques

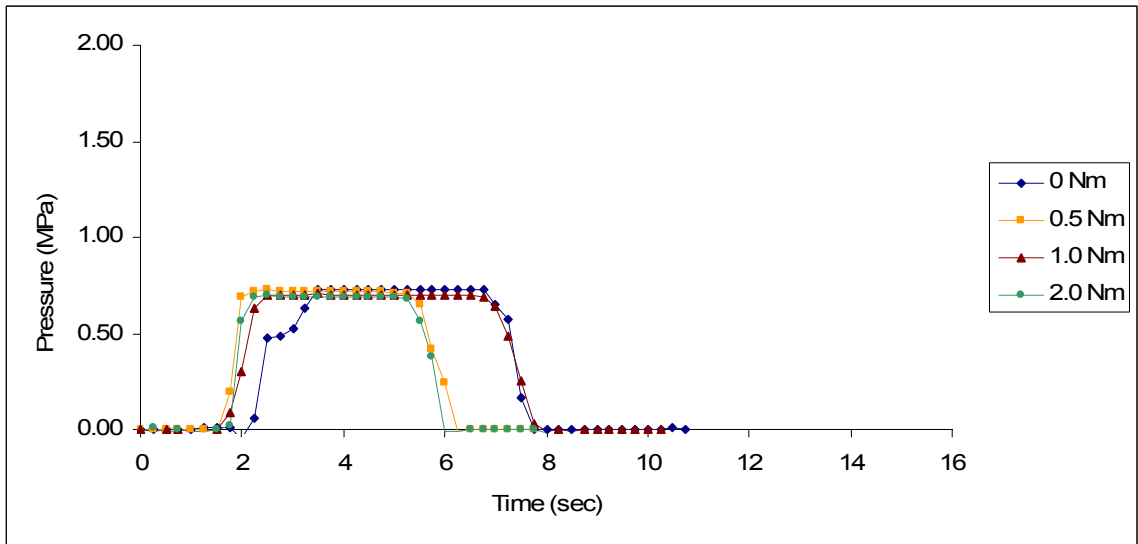


Figure 23 - Pressure of DBU UJ04J002 at Different Torques

Appendix B – (Continued)

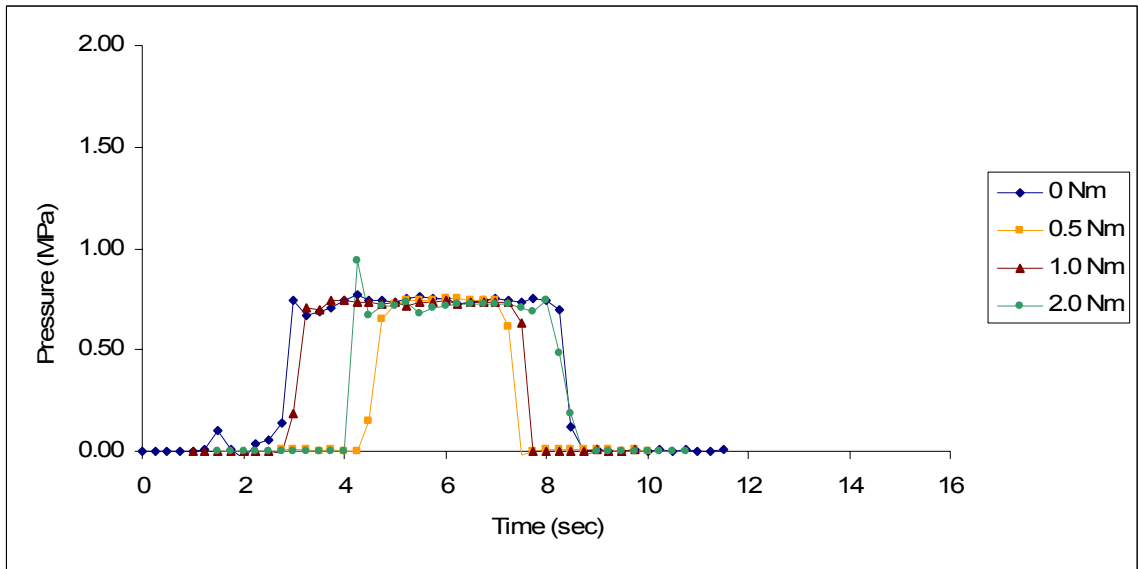


Figure 24 - Pressure of FSU UF05H007 at Different Torques

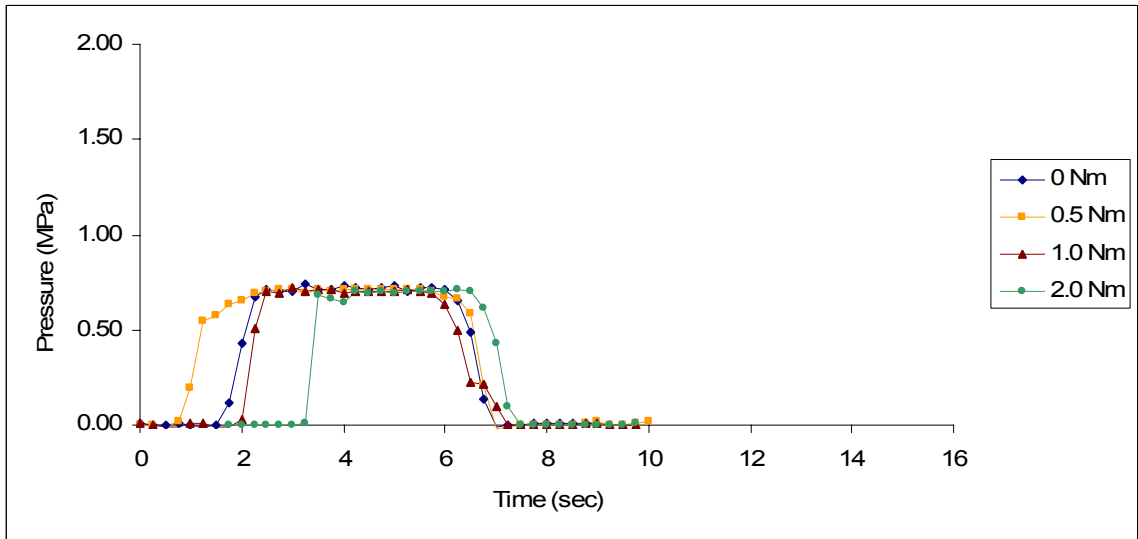


Figure 25 - Pressure of DBU UF05H007 at Different Torques

Appendix B – (Continued)

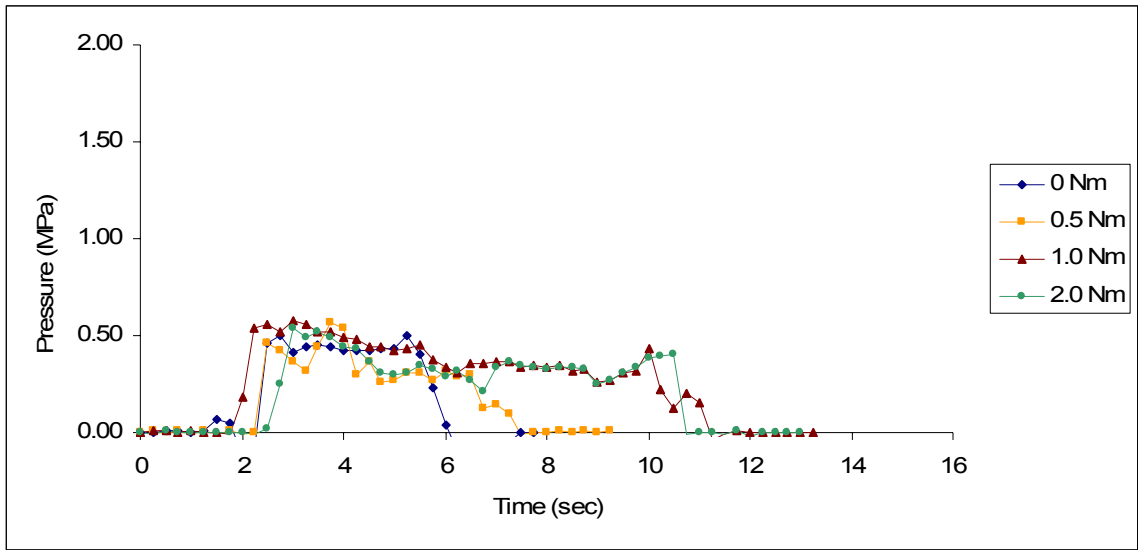


Figure 26 - Pressure of FSU UM05H007 at Different Torques

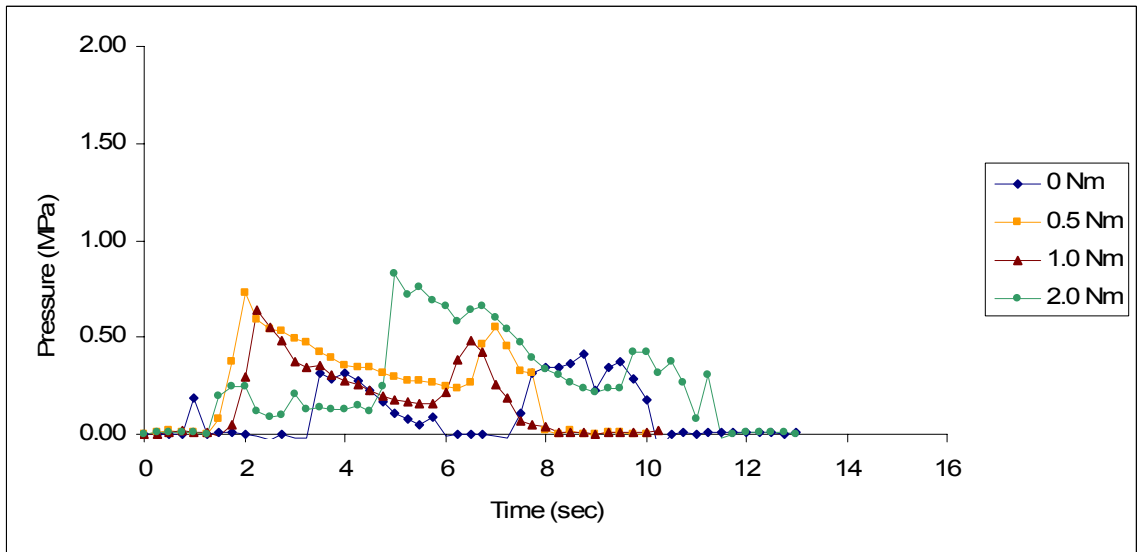


Figure 27 - Pressure of DBU UM05H007 at Different Torques

Appendix B – (Continued)

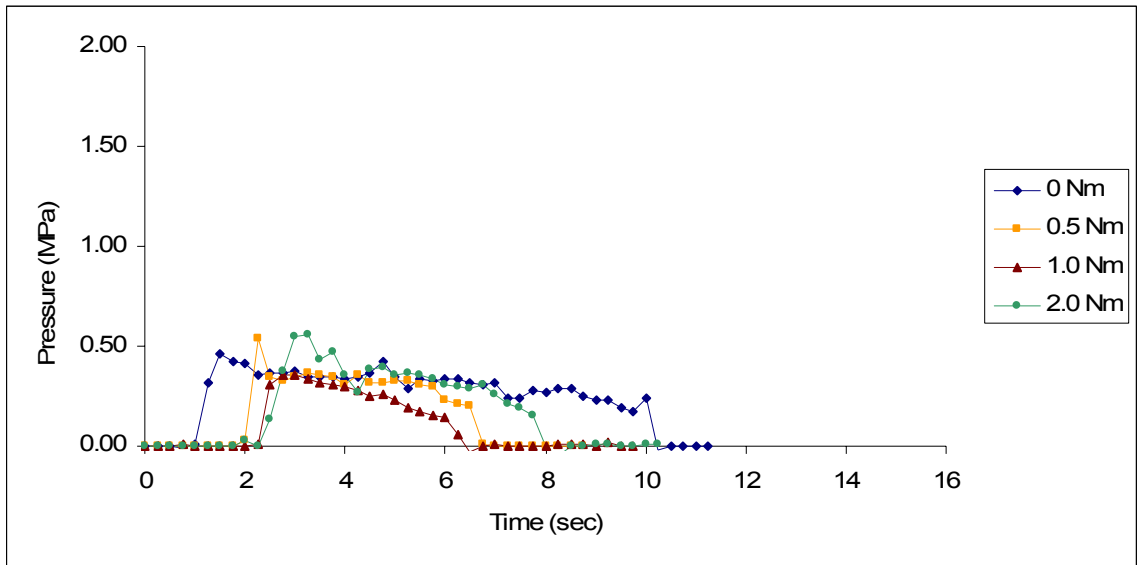


Figure 28 - Pressure of FSU UF05B003 at Different Torques

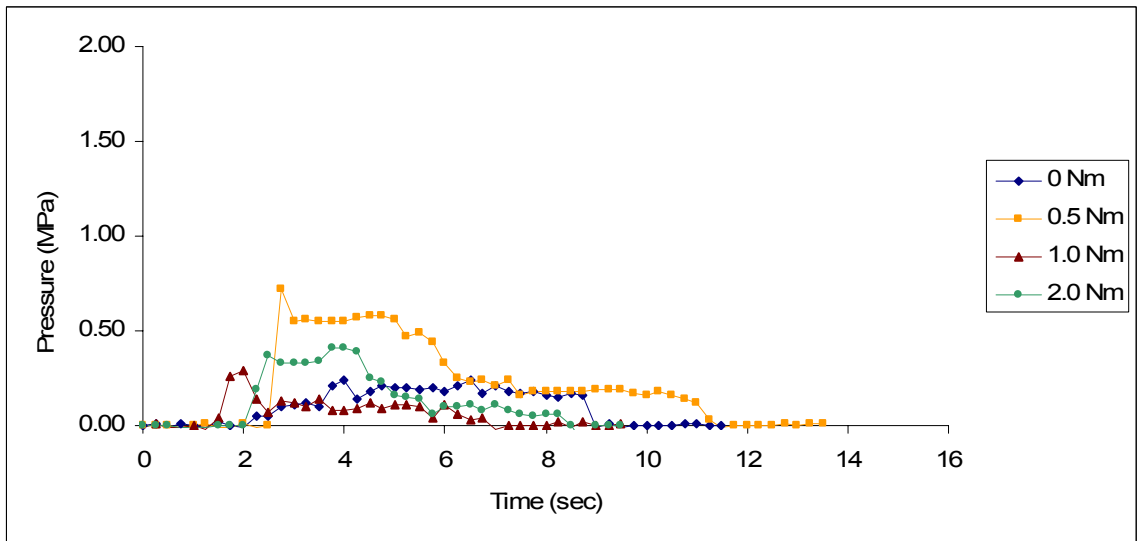


Figure 29 - Pressure of DBU UF05B003 at Different Torques

Appendix B – (Continued)

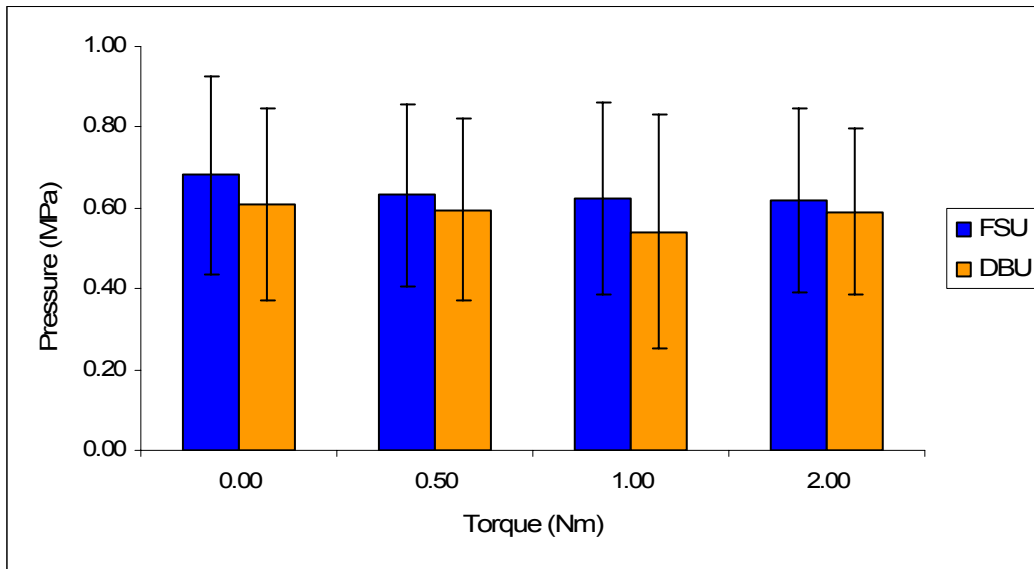


Figure 30 - Pressure Versus Torque of 6 FSU's and 6 DBU's (n=6). Results Shown in Mean \pm Standard Deviation

Appendix B – (Continued)

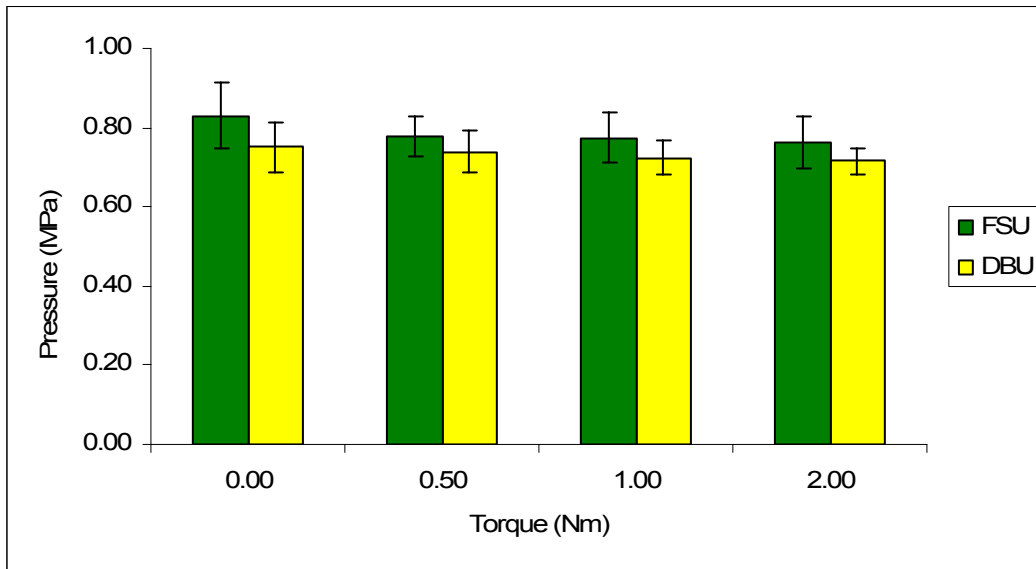


Figure 31 - Pressure Versus Torque of 4 FSU's and 4 DBU's (n=4). Results Shown in Mean \pm Standard Deviation

Appendix B – (Continued)

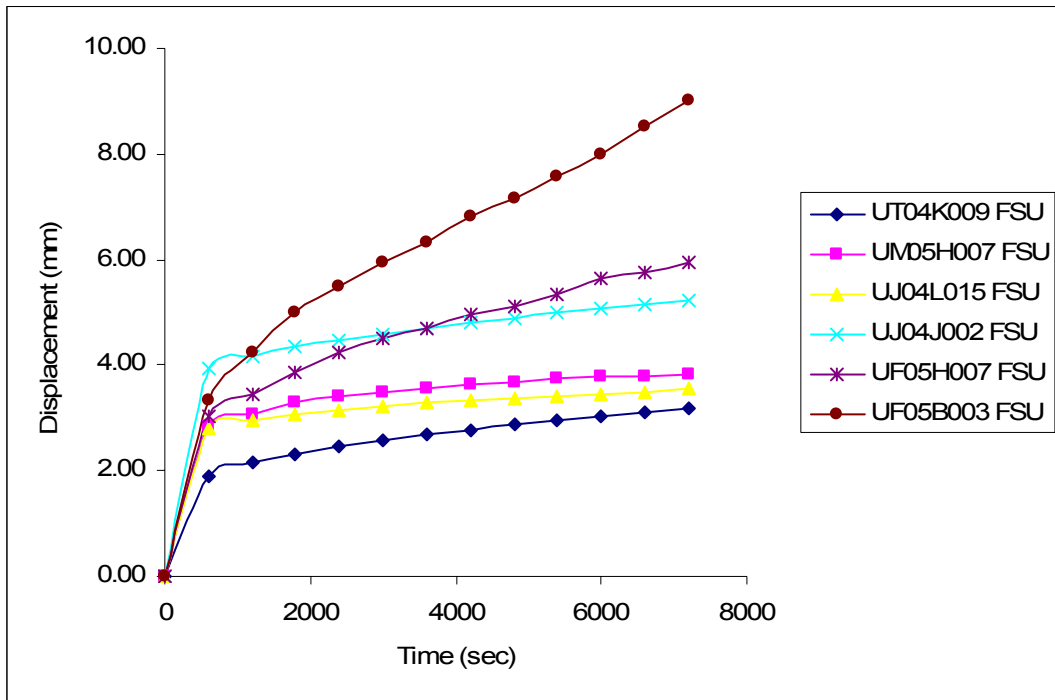


Figure 32 - FSU Two Hour Creep Curves

Appendix B – (Continued)

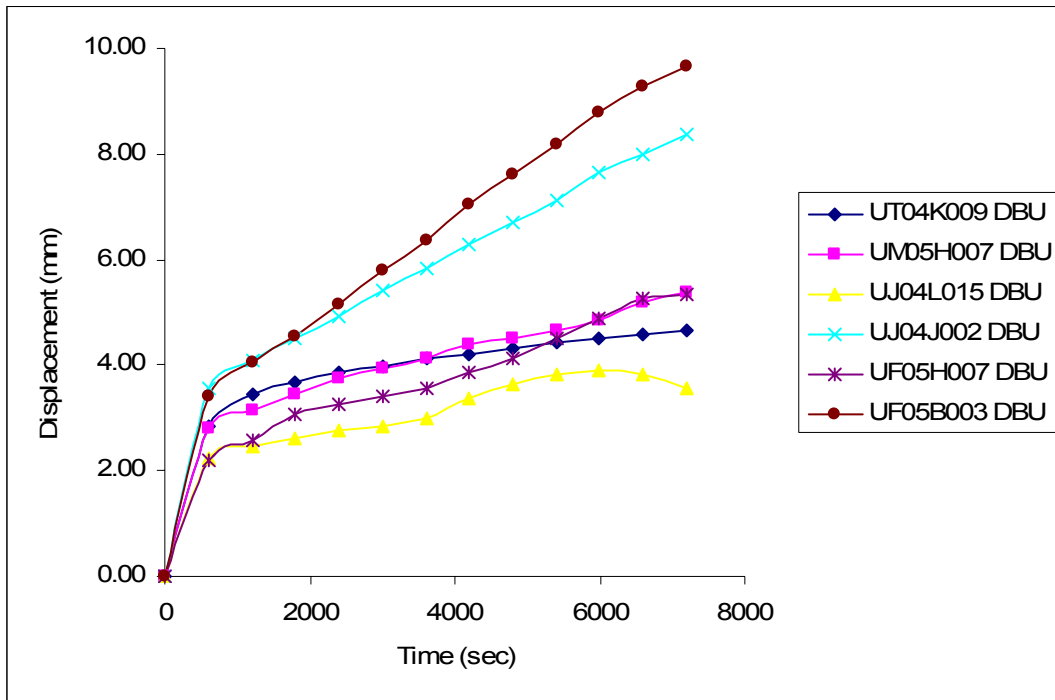


Figure 33 - DBU Two Hour Creep Curves

Appendix B – (Continued)

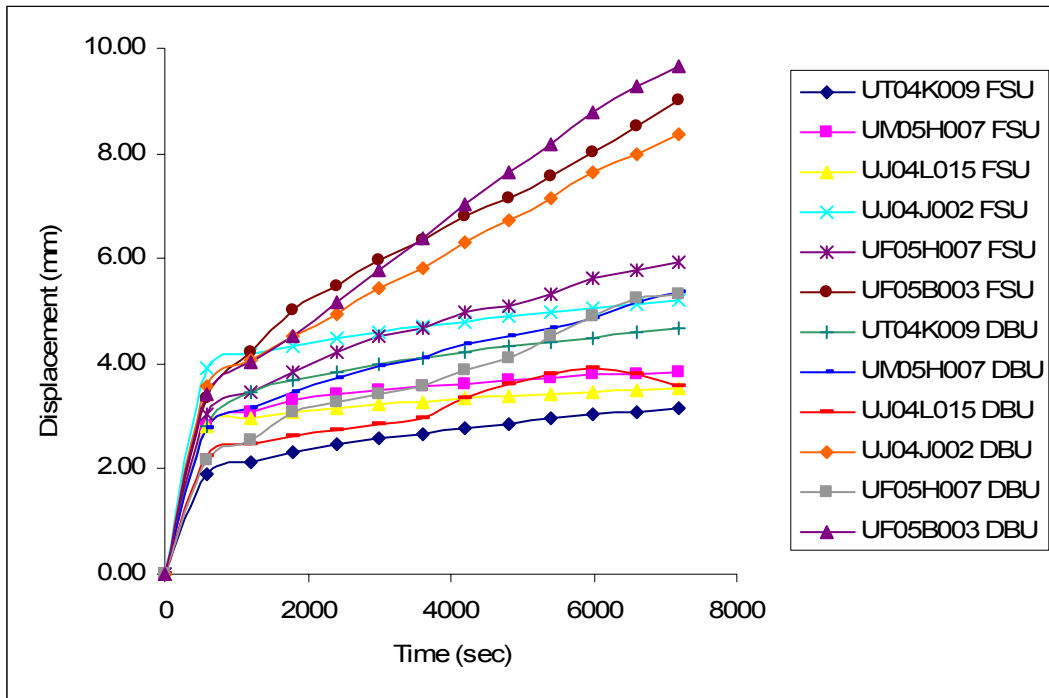


Figure 34 - Combined FSU and DBU Two Hour Creep Curves

Appendix B – (Continued)

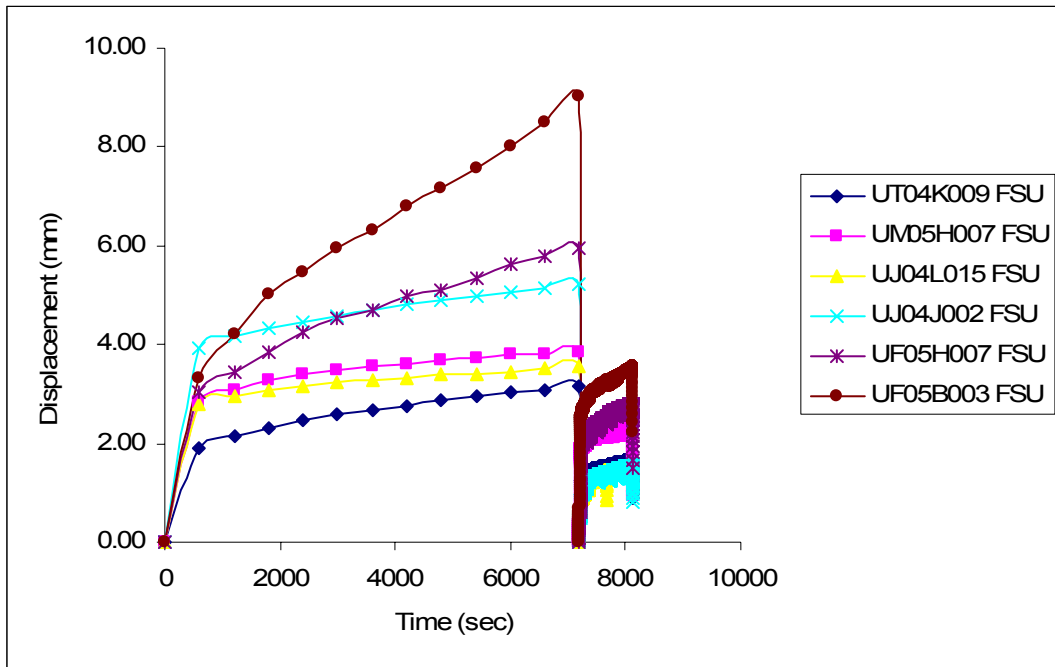


Figure 35 - Continuous FSU Creep Curves with Two Hour Creep and Testing

Appendix B – (Continued)

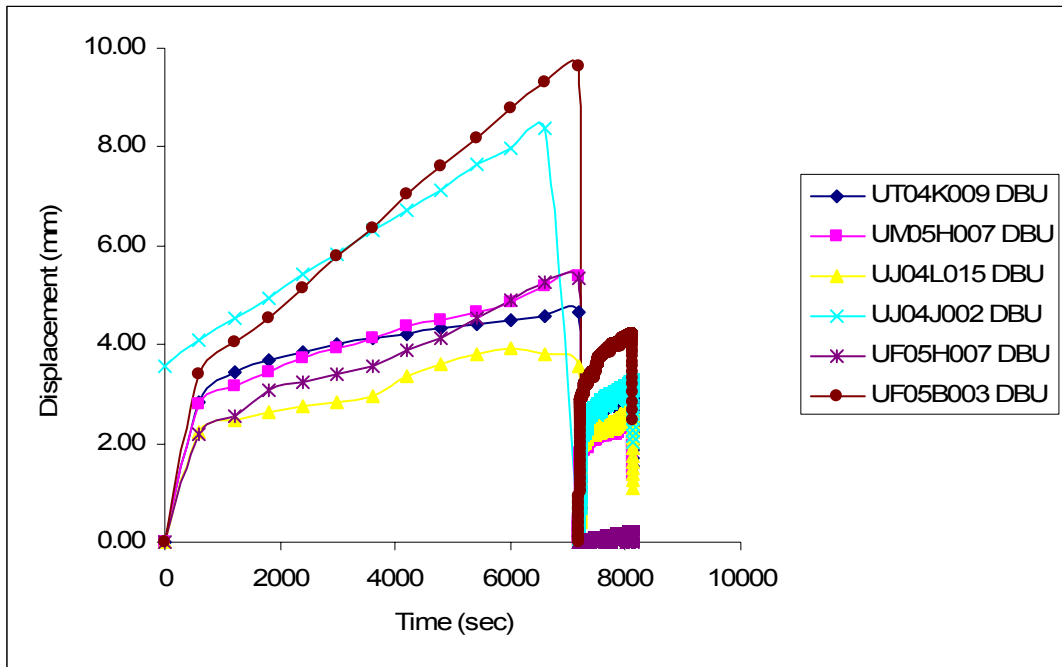


Figure 36 - Continuous DBU Creep Curves with Two Hour Creep and Testing

Appendix B – (Continued)

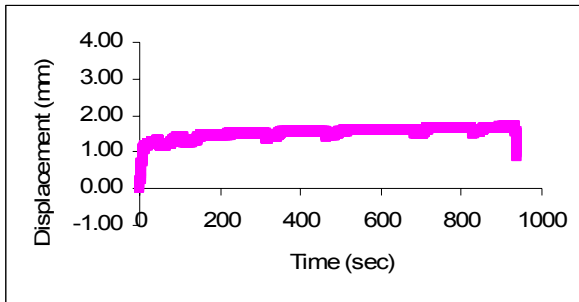


Figure 37 - Axial Displacement of FSU UT04K009

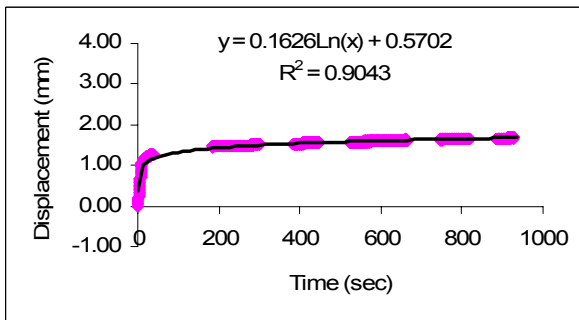


Figure 38 - Axial Displacement of FSU UT04K009 with Logarithmic Trendline

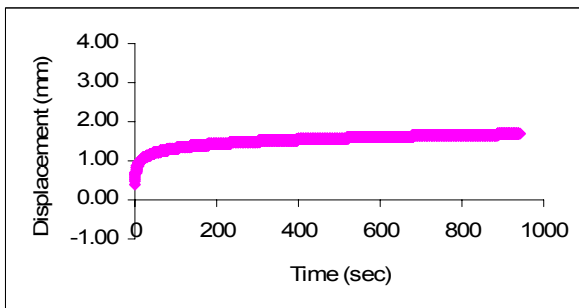


Figure 39 - Axial Displacement of FSU UT04K009 with Creep Only

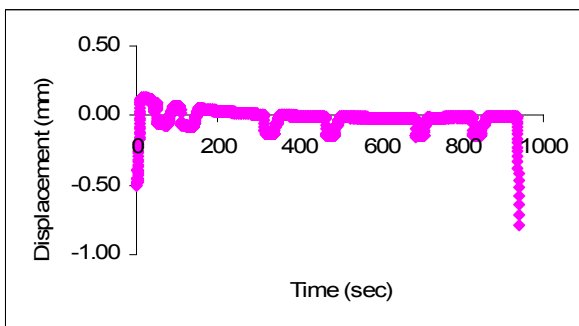


Figure 40 - Magnitude of the Height Differences of FSU UT04K009

Appendix B – (Continued)

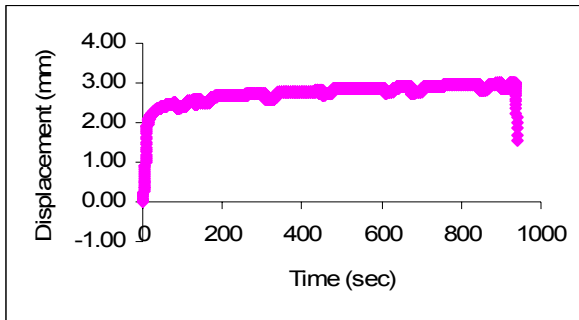


Figure 41 - Axial Displacement of DBU UT04K009

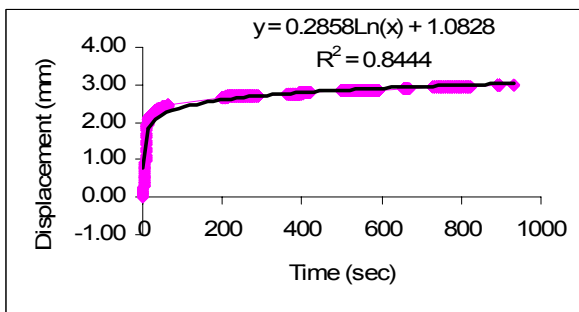


Figure 42 - Axial Displacement of DBU UT04K009 with Logarithmic Trendline

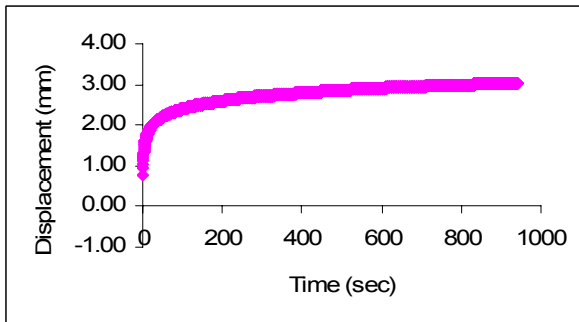


Figure 43 - Axial Displacement of DBU UT04K009 with Creep Only

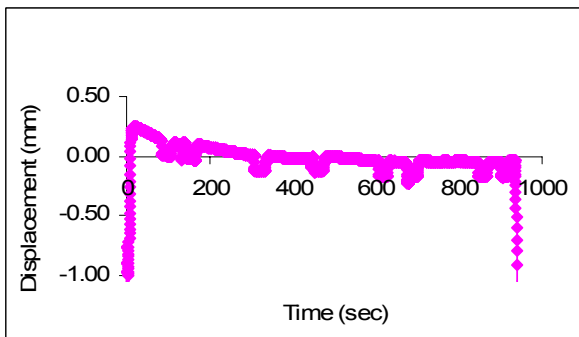


Figure 44 - Magnitude of the Height Differences of DBU UT04K009

Appendix B – (Continued)

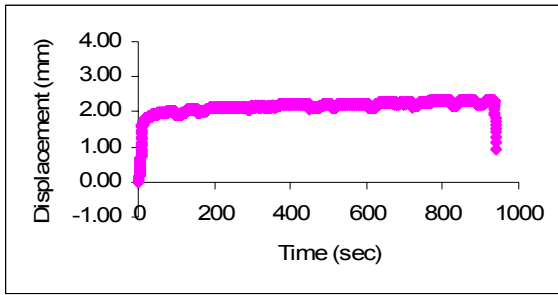


Figure 45 - Axial Displacement of FSU UM05H007

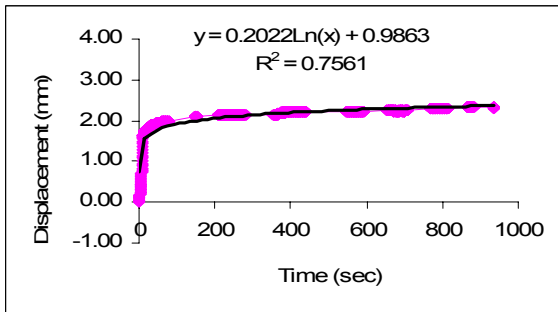


Figure 46 - Axial Displacement of FSU UM05H007 with Logarithmic Trendline

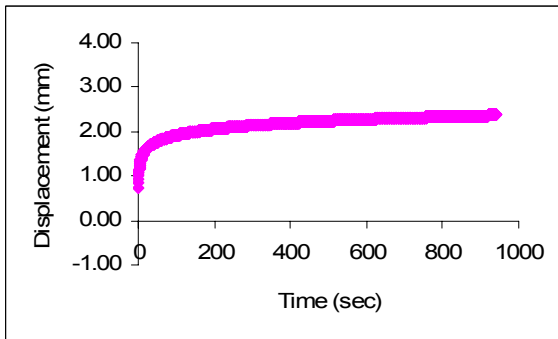


Figure 47 - Axial Displacement of FSU UM05H007 with Creep Only

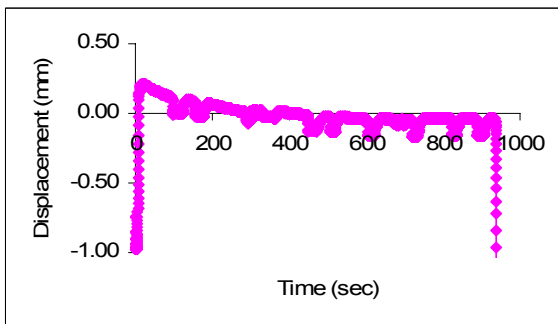


Figure 48 - Magnitude of the Height Differences of FSU UM05H007

Appendix B – (Continued)

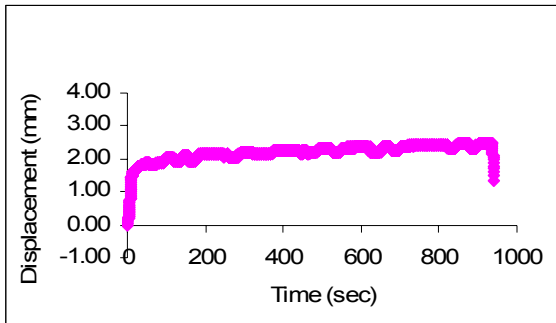


Figure 49 - Axial Displacement of DBU UM05H007

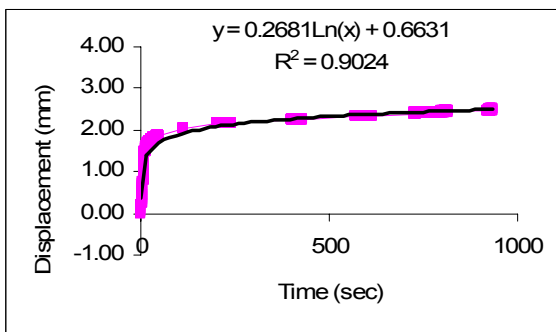


Figure 50 - Axial Displacement of DBU UM05H007 with Logarithmic Trendline

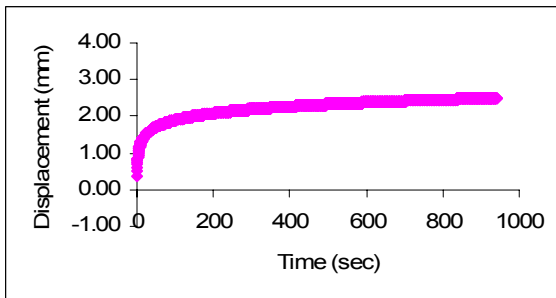


Figure 51 - Axial Displacement of DBU UM05H007 with Creep Only

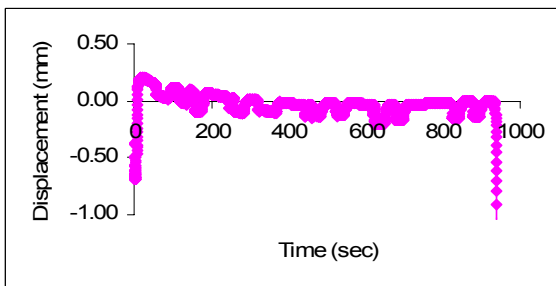


Figure 52 - Magnitude of the Height Differences of DBU UM05H007

Appendix B – (Continued)

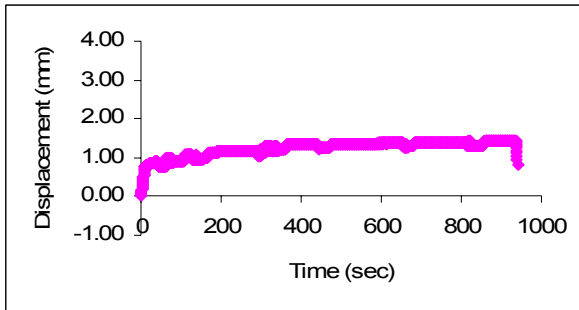


Figure 53 - Axial Displacement of FSU UJ04L015

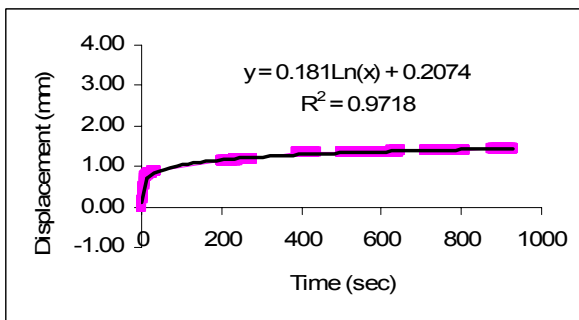


Figure 54 - Axial Displacement of FSU UJ04L015 with Logarithmic Trendline

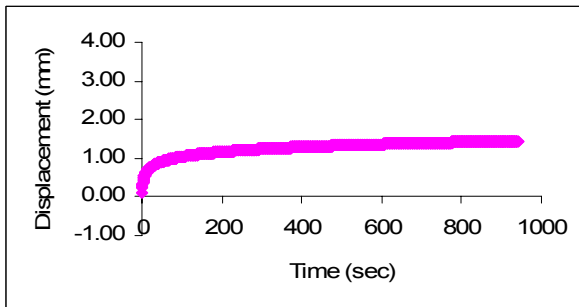


Figure 55 - Axial Displacement of FSU UJ04L015 with Creep Only

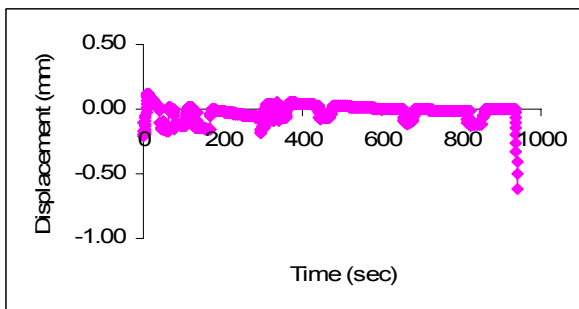


Figure 56 - Magnitude of the Height Differences of FSU UJ04L015

Appendix B – (Continued)

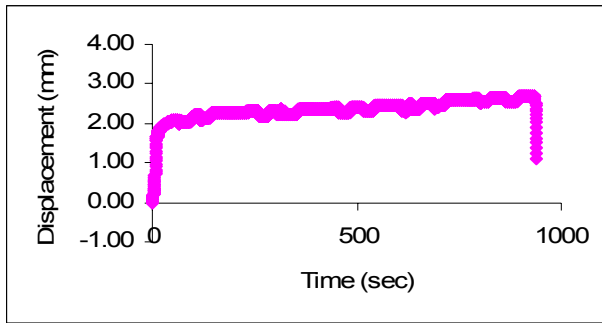


Figure 57 - Axial Displacement of DBU UJ04L015

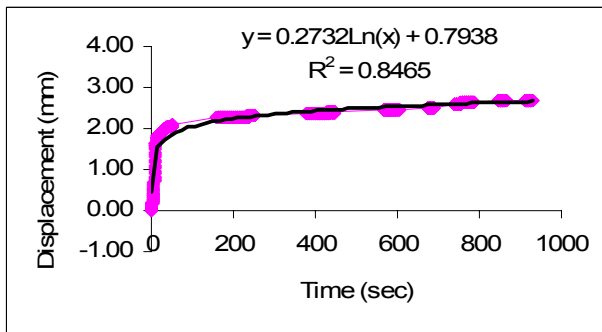


Figure 58 - Axial Displacement of DBU UJ04L015 with Logarithmic Trendline

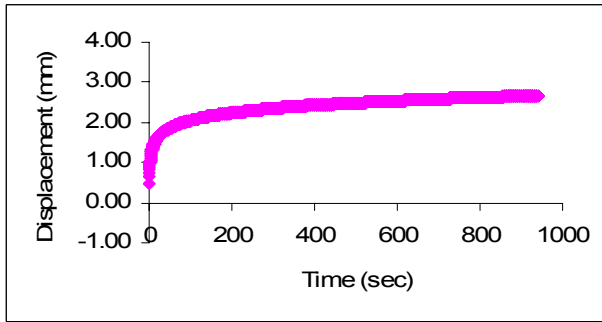


Figure 59 - Axial Displacement of DBU UJ04L015 with Creep Only

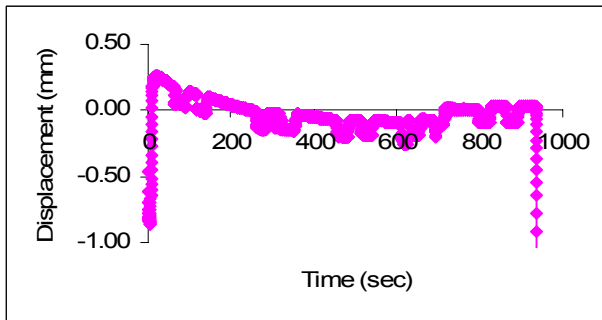


Figure 60 - Magnitude of the Height Differences of DBU UJ04L015

Appendix B – (Continued)

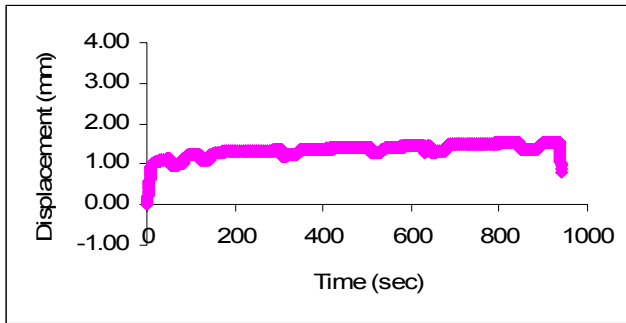


Figure 61 - Axial Displacement of FSU UJ04J002

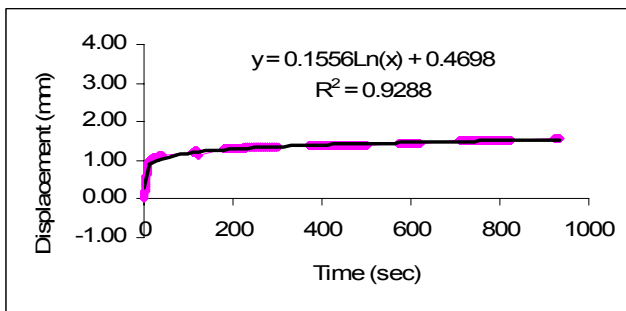


Figure 62 - Axial Displacement of FSU UJ04J002 with Logarithmic Trendline

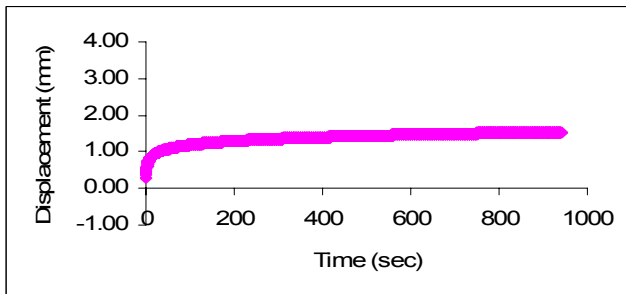


Figure 63 - Axial Displacement of FSU UJ04J002 with Creep Only

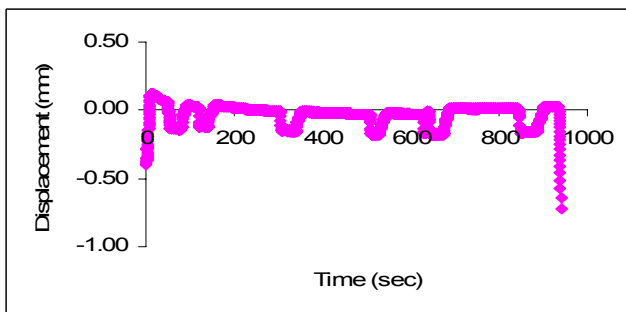


Figure 64 - Magnitude of the Height Differences of FSU UJ04J002

Appendix B – (Continued)

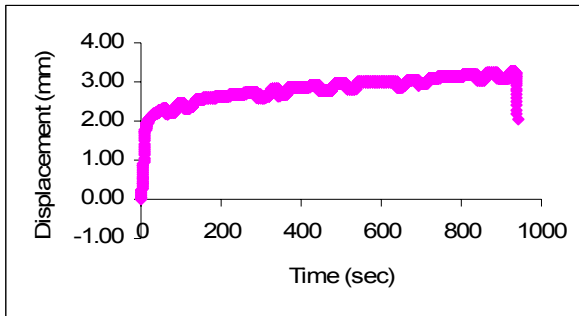


Figure 65 - Axial Displacement of DBU UJ04J002

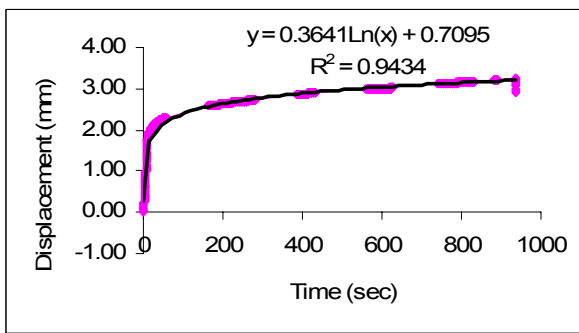


Figure 66 - Axial Displacement of DBU UJ04J002 with Logarithmic Trendline

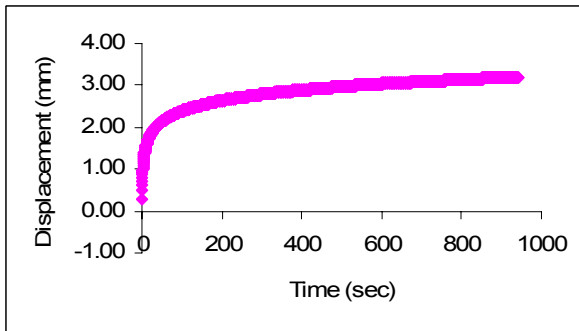


Figure 67 - Axial Displacement of DBU UJ04J002 with Creep Only

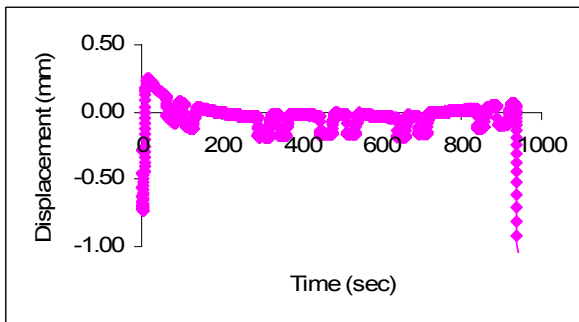


Figure 68 - Magnitude of the Height Differences of DBU UJ04J002

Appendix B – (Continued)

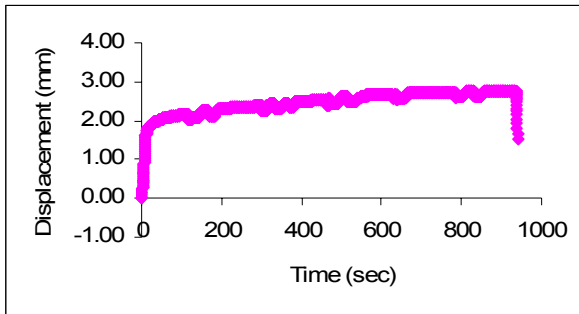


Figure 69 - Axial Displacement of FSU UF05H007

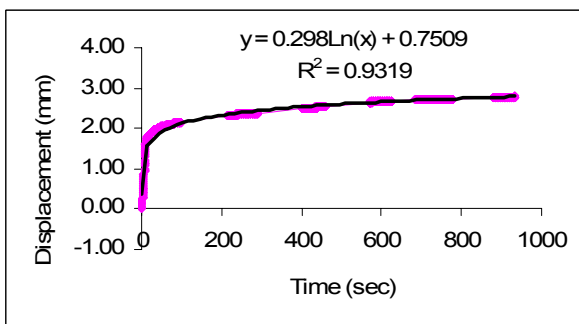


Figure 70 - Axial Displacement of FSU UF05H007 with Logarithmic Trendline

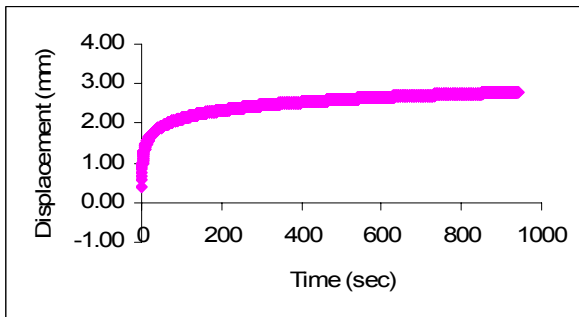


Figure 71 - Axial Displacement of FSU UF05H007 with Creep Only

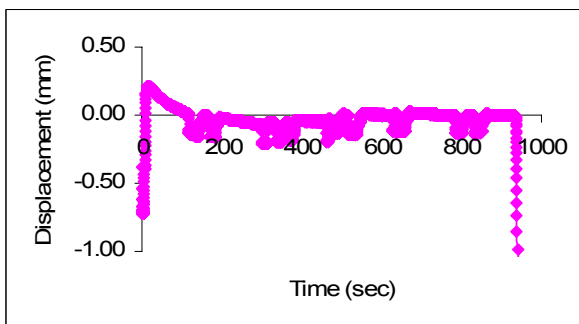


Figure 72 - Magnitude of the Height Differences of FSU UF05H007

Appendix B – (Continued)

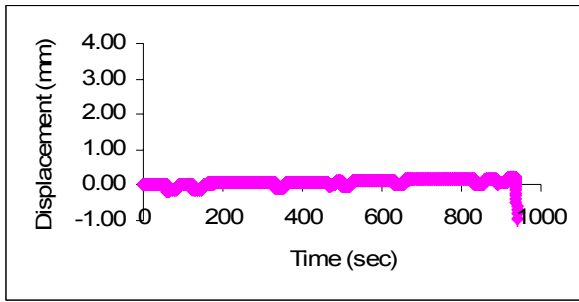


Figure 73 - Axial Displacement of DBU UF05H007

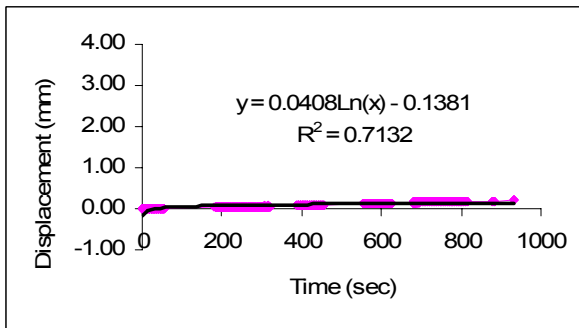


Figure 74 - Axial Displacement of DBU UF05H007 with Logarithmic Trendline

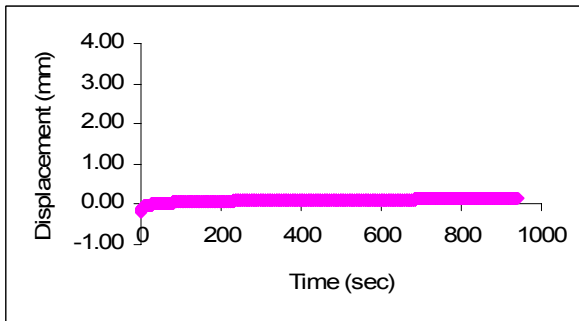


Figure 75 - Axial Displacement of DBU UF05H007 with Creep Only

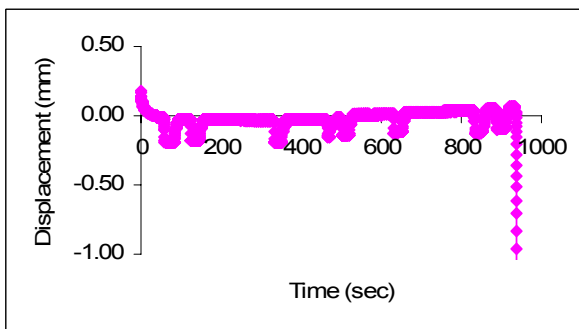


Figure 76 - Magnitude of the Height Differences of DBU UF05H007

Appendix B – (Continued)

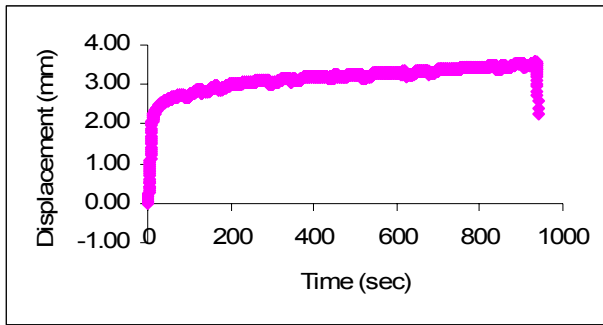


Figure 77 - Axial Displacement of FSU UF05B003

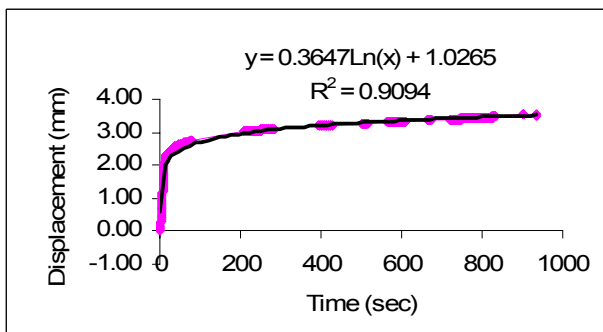


Figure 78 - Axial Displacement of FSU UF05B003 with Logarithmic Trendline

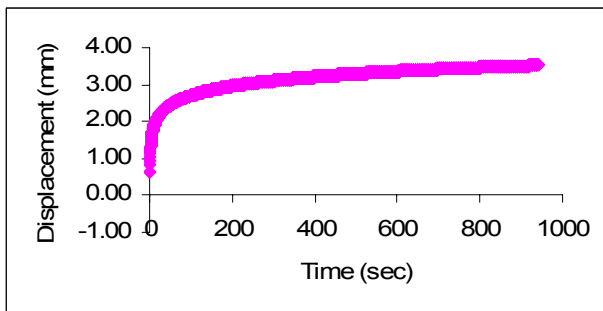


Figure 79 - Axial Displacement of FSU UF05B003 with Creep Only

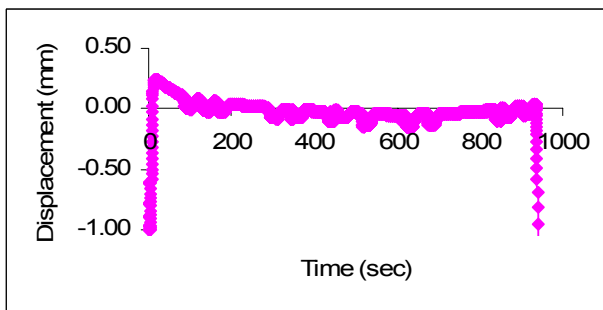


Figure 80 - Magnitude of the Height Differences of FSU UF05B003

Appendix B – (Continued)

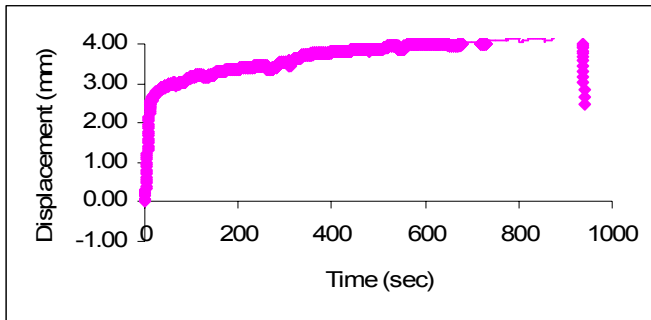


Figure 81 - Axial Displacement of DBU UF05B003

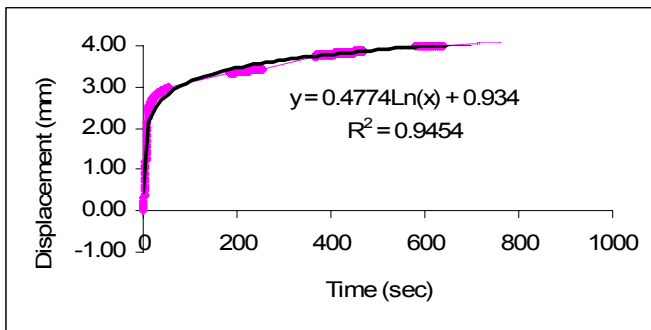


Figure 82 - Axial Displacement of DBU UF05B003 with Logarithmic Trendline

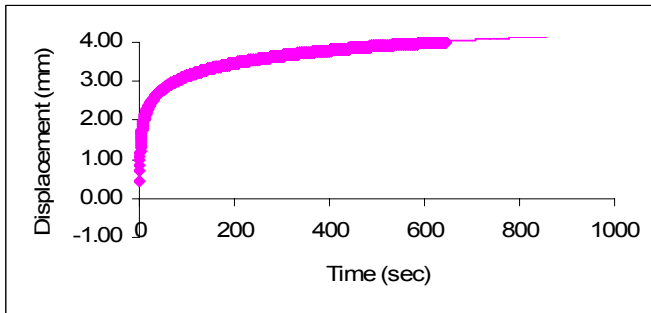


Figure 83 - Axial Displacement of DBU UF05B003 with Creep Only

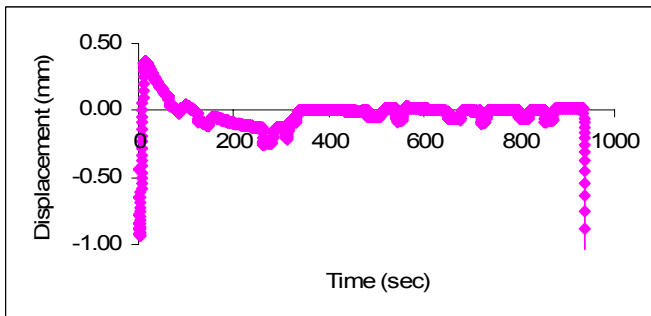


Figure 84 - Magnitude of the Height Differences of DBU UF05B003

Appendix B – (Continued)

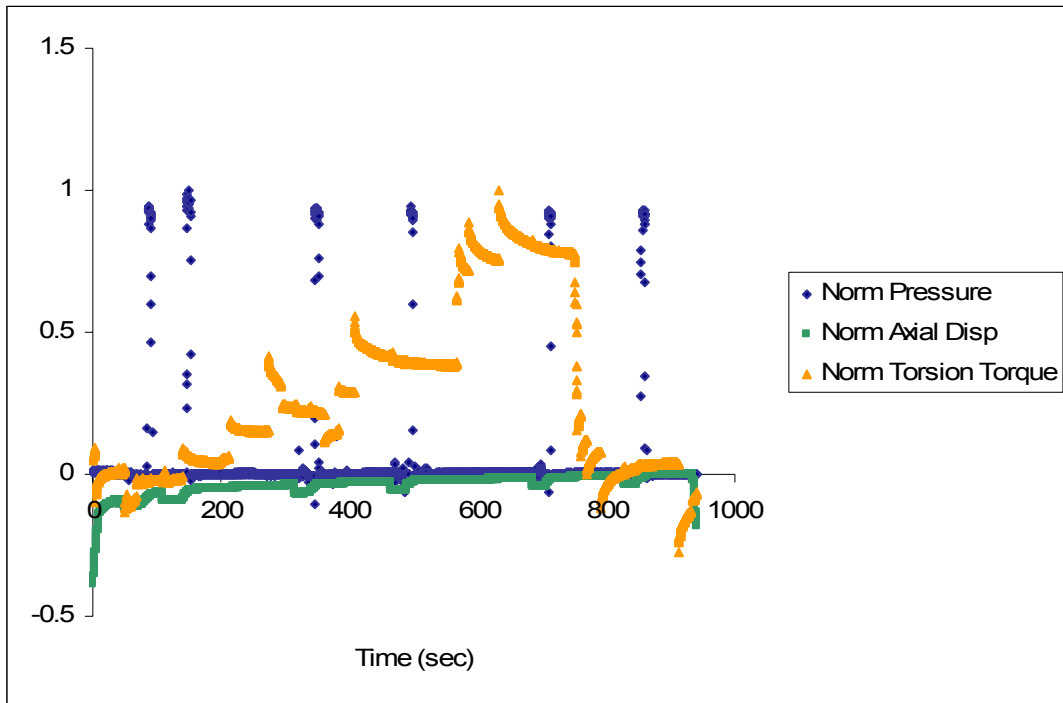


Figure 85 - Normalized Data Versus Time of FSU UT04K009

Appendix B – (Continued)

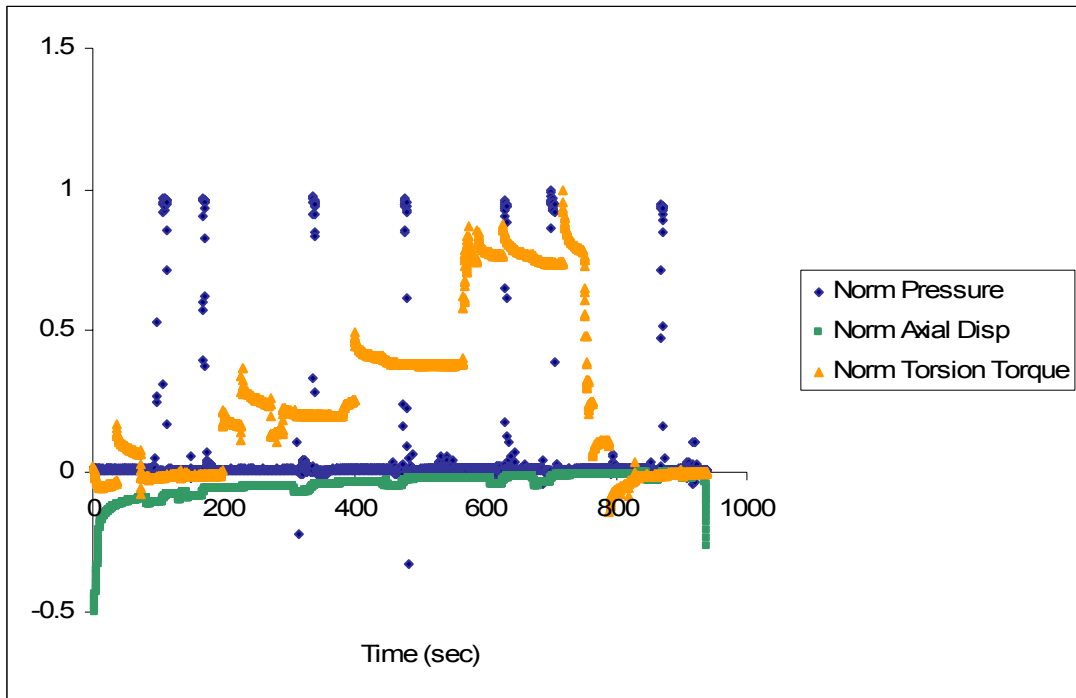


Figure 86 - Normalized Data Versus Time of DBU UT04K009

Appendix B – (Continued)

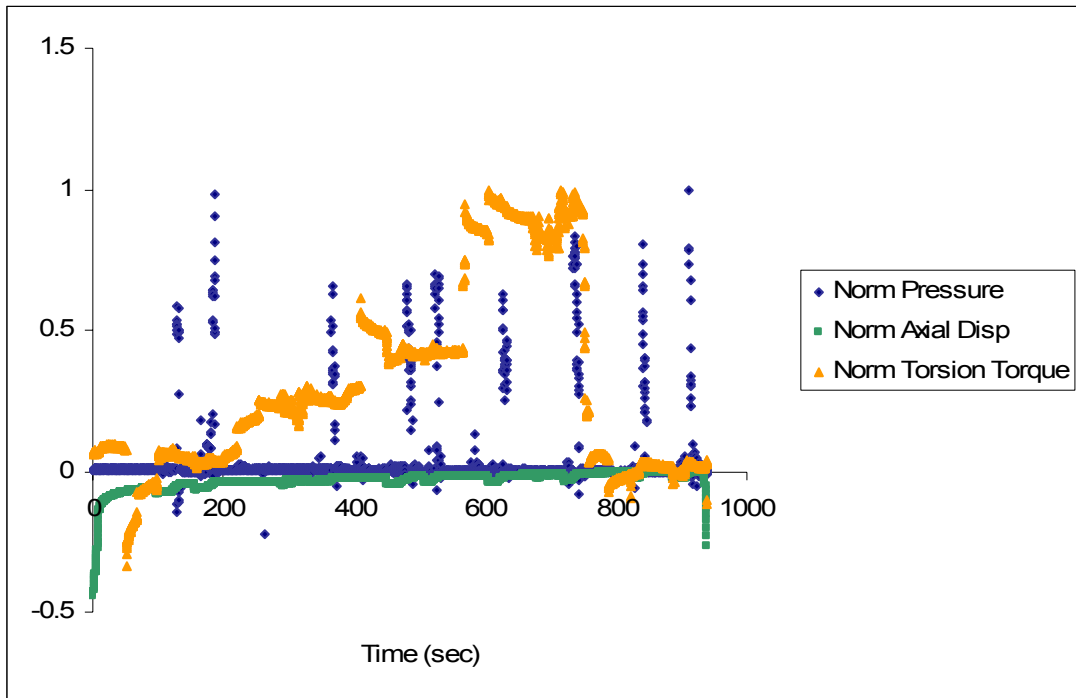


Figure 87 - Normalized Data Versus Time of FSU UM05H007

Appendix B – (Continued)

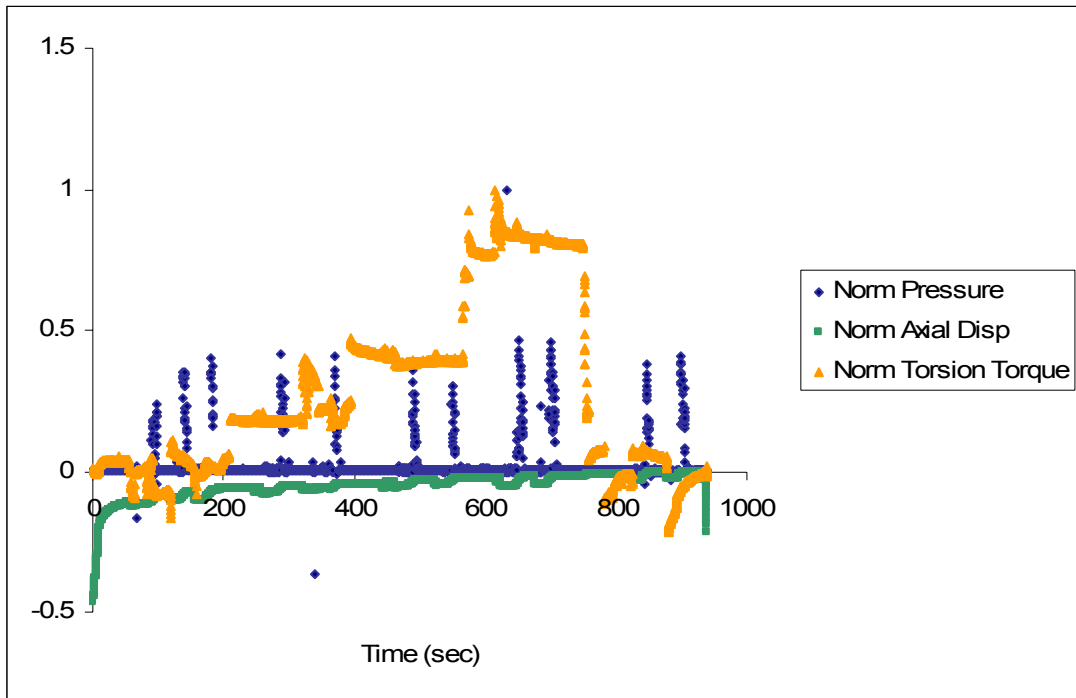


Figure 88 - Normalized Data Versus Time of DBU UM05H007

Appendix B – (Continued)

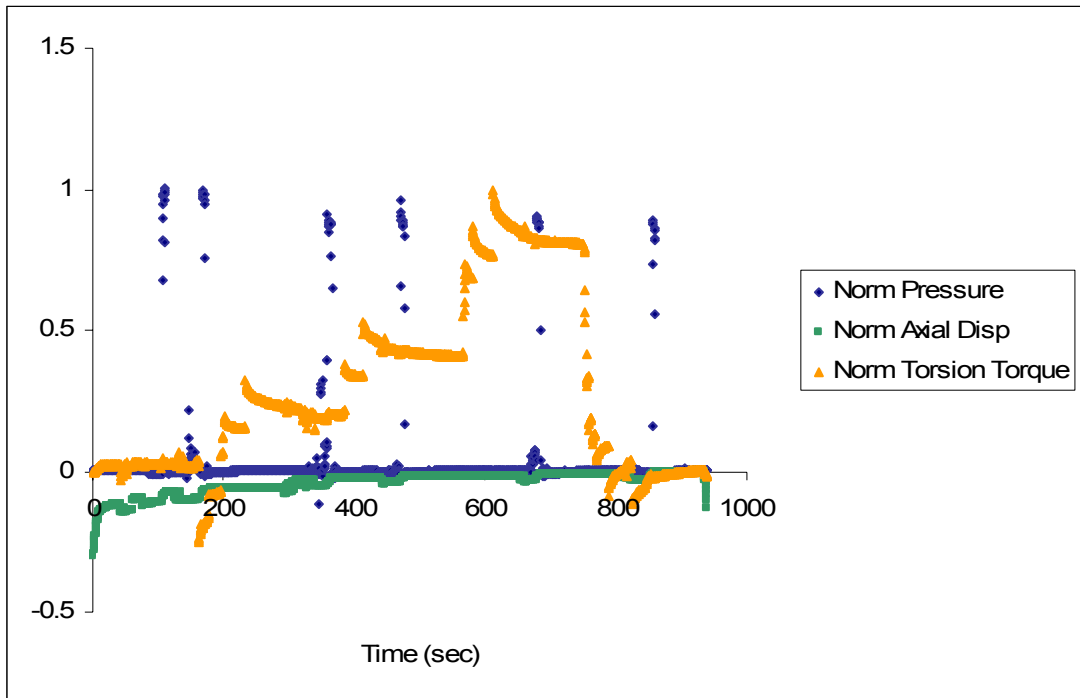


Figure 89 - Normalized Data Versus Time of FSU UJ04L015

Appendix B – (Continued)

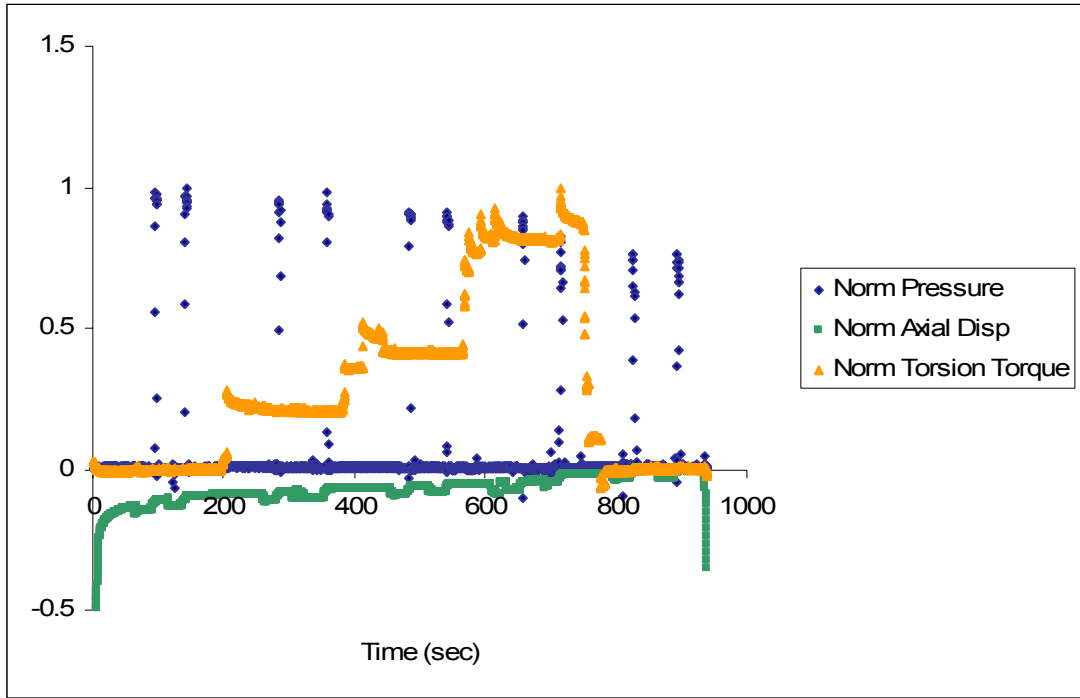


Figure 90 - Normalized Data Versus Time of DBU UJ04L015

Appendix B – (Continued)

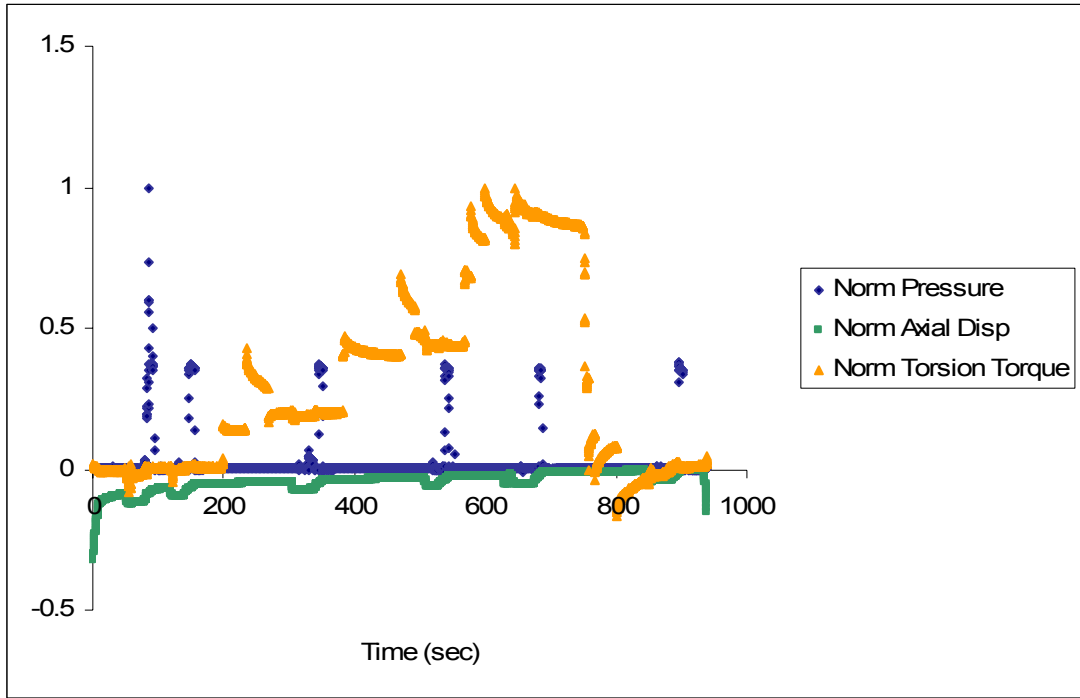


Figure 91 - Normalized Data Versus Time of FSU UJ04J002

Appendix B – (Continued)

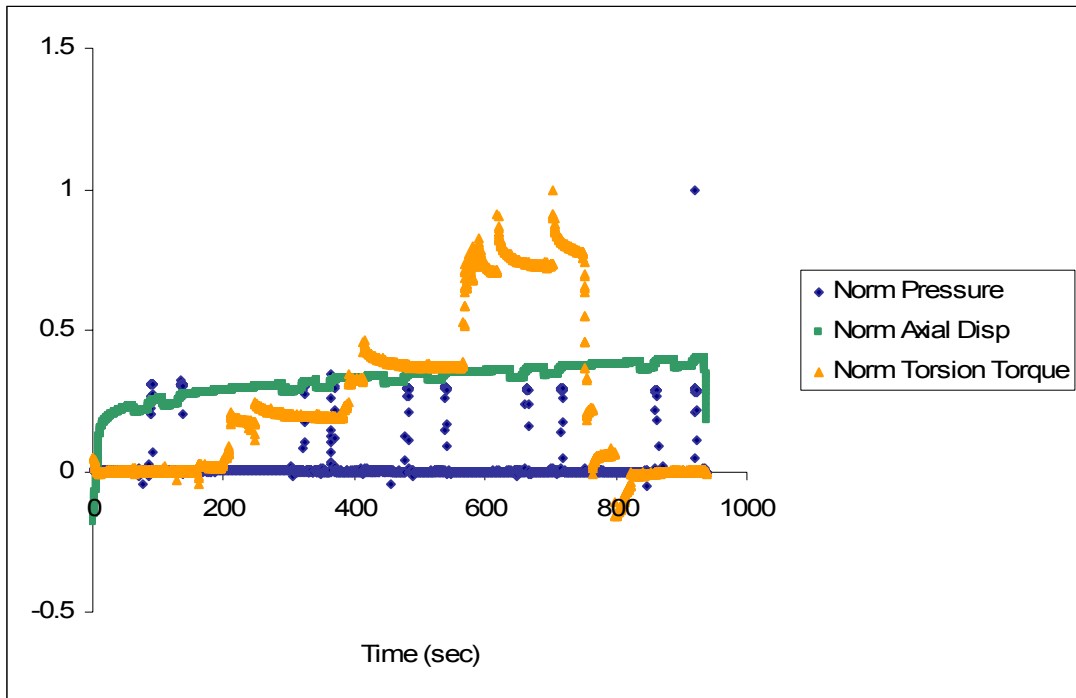


Figure 92 - Normalized Data Versus Time of DBU UJ04J002

Appendix B – (Continued)

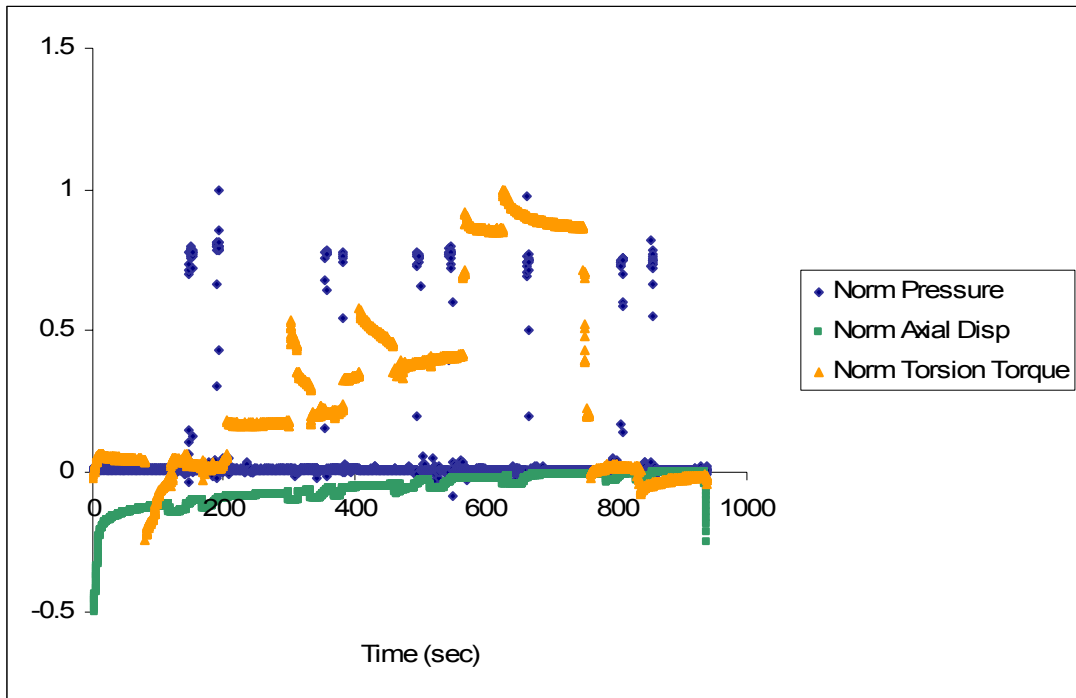


Figure 93 - Normalized Data Versus Time of FSU UF05H007

Appendix B – (Continued)

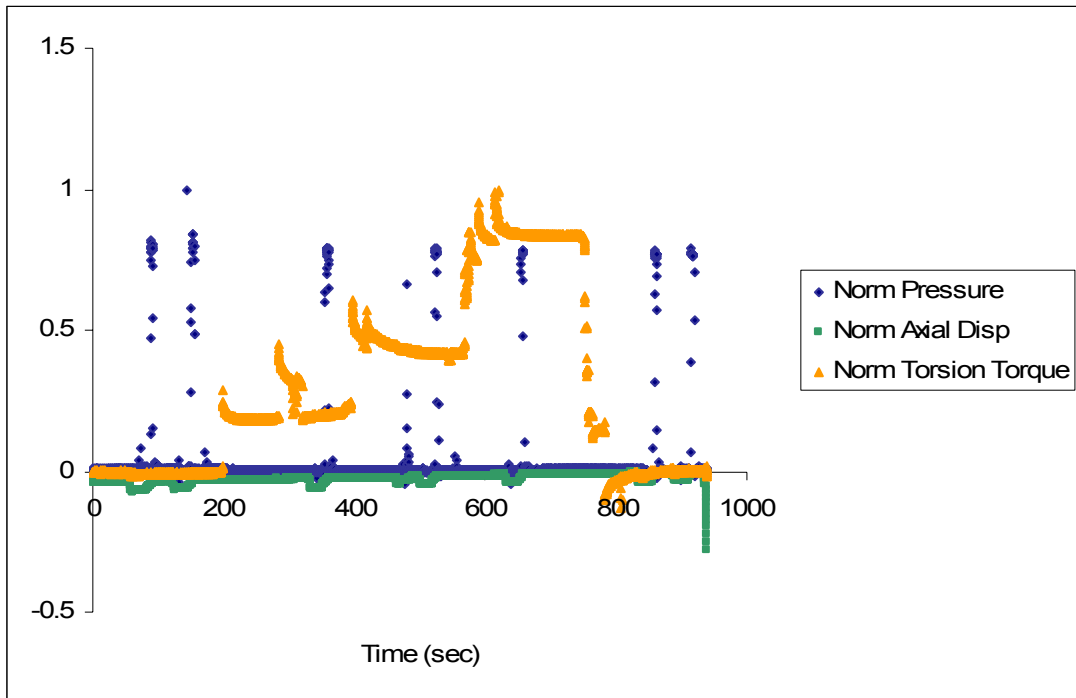


Figure 94 - Normalized Data Versus Time of DBU UF05H007

Appendix B – (Continued)

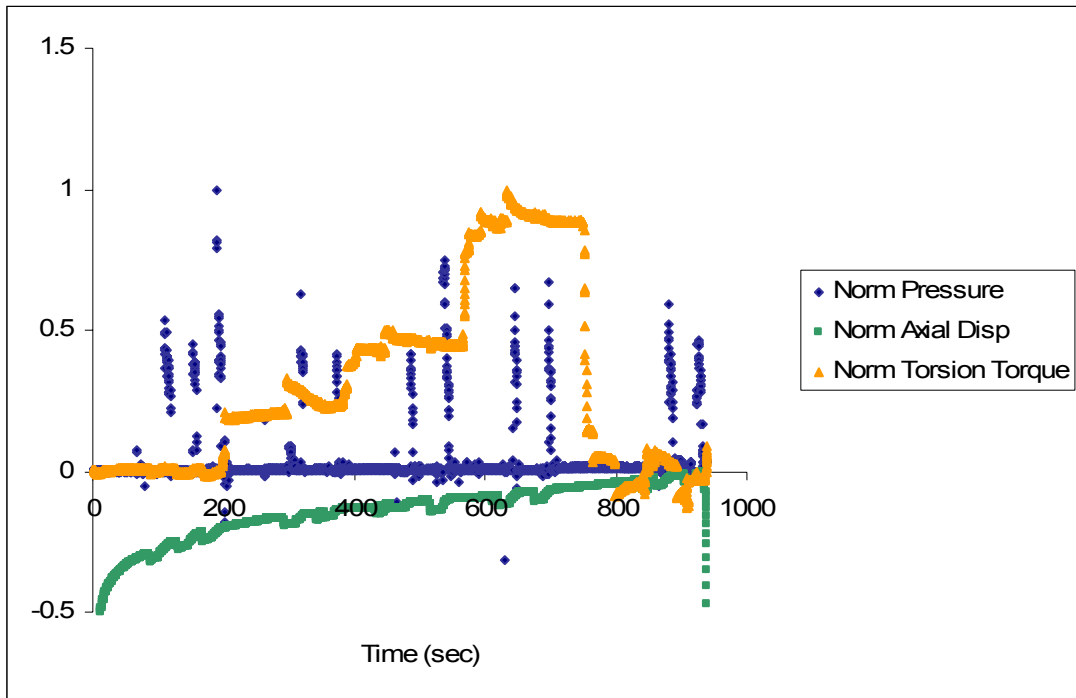


Figure 95 - Normalized Data Versus Time of FSU UF05B003

Appendix B – (Continued)

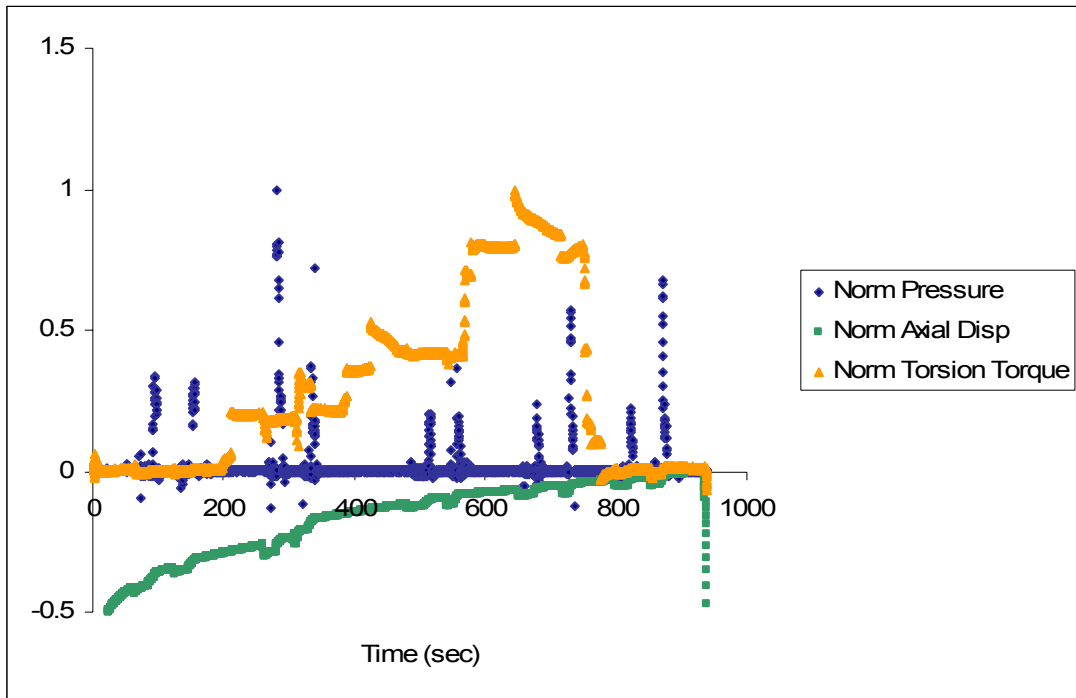


Figure 96 - Normalized Data Versus Time of DBU UF05B003

Appendix B – (Continued)

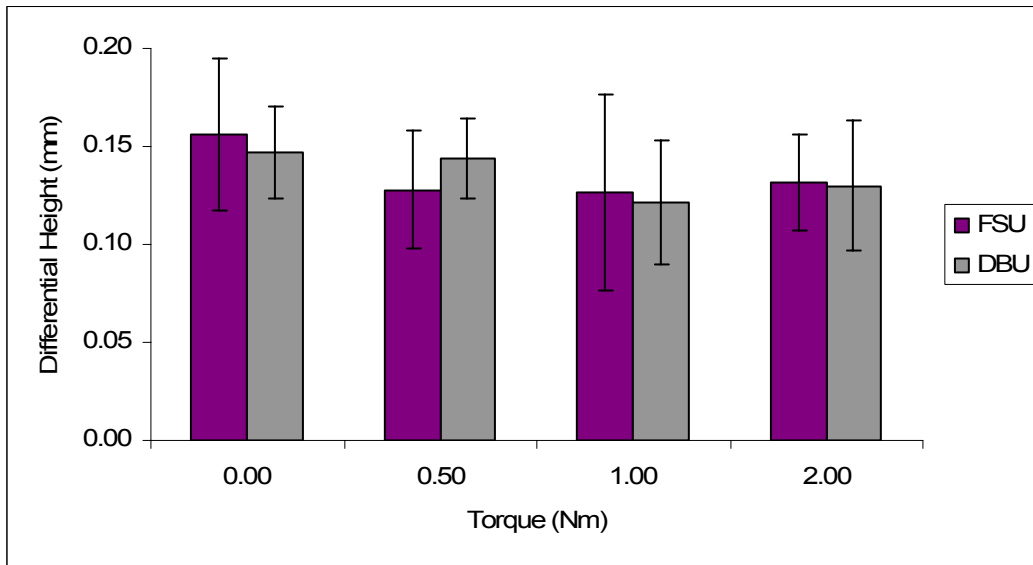


Figure 97 - Differential Height Versus Torque of 6 FSU's and 6 DBU's (n=6).
Results Shown in Mean \pm Standard Deviation